centas in SRS patients, except for our report documenting placental hypoplasia in three upd(7)mat patients [16]. In addition, further studies are necessary to confirm the reduced *IGF2* expression level and to examine the relevance of KvDMR1 hypermethylation to SRS. Similarly, while phenotypic difference has been suggested between the *H19*-DMR epimutation-positive and epimutation-negative patients [5, 6], this notion awaits further investigation. Thus, we studied the methylation status of the *H19*-DMR and the KvDMR1, expression status of *IGF2* and *H19*, and clinical phenotypes of bodies and placentas in SRS patients. Furthermore, we also analyzed correlations among molecular and clinical data. The results reveal characteristic molecular and clinical findings and their correlations in both the bodies and the placentas of SRS patients.

Materials and methods

Patients

We studied 60 Japanese patients (31 males and 29 females) with the SRS phenotype aged 0–30 years (median 6.5 years). The selection criteria used were (1) prenatal growth failure (birth length and/or weight <−2.0 SD for gestational age) plus at least three of the following five features: postnatal growth failure (stature <−2.0 SD at 2 years of age or at the last examination), relative macrocephaly, triangular face, hemihypotrophy, and clinodactyly; (2) no discernible endocrine or skeletal disorders; (3) normal karyotype in all the ≥50 lymphocytes examined; and (4) exclusion of upd(7)mat accounting for 7–10% of SRS [1], and upd(14)mat associated with pre- and postnatal growth failure [24] by PCR-based methylation analysis for the *MEST*-DMR on 7q32.2 and the *MEG3*-DMR on 14q32.2, respectively, using methylated and unmethylated allele-specific primers (three patients were found to have upd(7)mat by this screening) [16, 18]. This study was approved by the Institutional Review Board Committee at the National Center for Child health and Development, and written informed consent was obtained from each subject or the parent(s).

Extraction of DNA and RNA samples

Leukocyte genomic DNA was obtained with FlexiGene DNA Kit (Qiagen, Valencia, CA, USA), and RNA was prepared with RNeasy Plus Mini (Qiagen). Genomic DNA and RNA from paraffin-embedded placental samples were extracted with RecoverAll Total Nucleic Acids Isolation Kit (Ambion, Austin, TX, USA) using slices of 40-μm thick.

Methylation analysis

Combined bisulfite restriction analysis (COBRA) and bisulfite sequencing were performed for genomic DNA treated with the EZ DNA Methylation Kit (Zymo Research, Orange, CA, USA) that converts all the cytosines except for methylated cytosines at the CpG dinucleotides into uracils and subsequently thymines. The primers used are shown in Supplementary Table 1.

For COBRA, the *H19*-DMR and the KvDMR1 were amplified with primer sets that hybridize to both methylated and unmethylated alleles because of absent CpG dinucleotides within the primer sequences, and the PCR products were digested with methylated allele-specific restriction enzymes (*Bsa*BI and *Mwo*I for the *H19*-DMR; *Hpy*188I and *Eci*I for the KvDMR1; Fig. 1a). Although the *H19*-DMR examined in this study is outside the CTCF binding sites, this region has been shown to be a DMR in leukocytes [25]. Subsequently, the digests were loaded onto a DNA 1000 LabChip and assayed using the 2100 Bioanalyzer (Agilent, Santa Clara, CA, USA). To allow for quantitative assessment, the ratio of methylated clones (the methylation index) was obtained using peak heights of digested and undigested fragments calculated by the 2100 expert software (Agilent; the Bio-COBRA method) [26]. To define the normal range for the methylation indices, 40 control subjects were similarly studied. The values below and above the normal range were regarded as hypomethylation and hypermethylation, respectively.

For bisulfite sequencing, the PCR products were subcloned with TOPO TA Cloning Kit (Invitrogen, Carlsbad, CA, USA), and multiple clones were subjected to direct sequencing on the CEQ 8000 autosequencer (Beckman Coulter, Fullerton, CA, USA). The T/G SNP (*rs2251375*) within the *H19*-DMR (Fig. 1a) was also genotyped by the sequencing.

Microsatellite analysis

Six loci on the distal 11p region were examined. A segment encompassing each locus was PCR-amplified with a fluorescently labeled forward primer and an unlabeled reverse primer and was determined for size on an ABI PRISM 310 autosequencer using GeneScan software (Applied Biosystems, Foster City, CA, USA). The primer sequences have been reported in the Human Genome Database (http://www.gdb.org/).

FISH analysis

Lymphocyte metaphase spreads were hybridized with a ~84-kb RP5-998N23 probe encompassing the *H19*-DMR, together with the CEP11 probe for the centromeric region of chromosome 11 used as an internal control. The RP5-998N23 was labeled with digoxigenin and detected by

rhodamine anti-digoxigenin, and the control probe was labeled with biotin and detected by avidin conjugated to fluorescein isothiocyanate.

Sequence analysis

The seven CTCF binding sites at the *H19*-DMR were subjected to direct sequencing on the autosequencer. The primer sequences were as reported previously [3].

Expression analysis

Expression levels and expression patterns of *IGF2* and *H19* were studied using leukocytes and placental samples. The primers used are shown in Supplementary Table 1.

To examine the expression levels, complementary DNA (cDNA) samples were synthesized from 500 ng of leukocytes and placental RNA using High Capacity cDNA Reverse Transcription Kit (Applied Biosystems). After DNase treatment using TURBO DNA-*free* Kit (Ambion), RT-PCR was performed with 20 ng of total RNA using AmpliTaq Gold DNA Polymerase (Applied Biosystems) with primers that were designed to span an intron to exclude possible genomic DNA contamination. After amplification, a small amount (1–2 μL) of reaction solutions was loaded onto a DNA 1000 LabChip and assayed using the Agilent 2100 Bioanalyzer after adjusting the *GAPDH* dosage among examined samples.

To examine expression patterns, leukocyte and placental cDNA and genomic DNA samples were subjected to direct sequencing using primers that were designed to amplify regions including exonic SNPs (*rs680* for *IGF2*; *rs2839703* and *rs2839704* for *H19*), together with parental leukocyte genomic DNA samples.

Data presentation and statistical analysis

After examining normality by the χ^2 test, the variables following the normal distribution were expressed as the mean ± SD, and those not following the normal distribution were expressed as the median (range). Statistical significance of the mean was analyzed by two-sided Student's *t* test for non-paired groups with similar variances, by two-sided paired *t* test for paired groups with similar variances, and by two-sided Welch's *t* test for non-paired groups with different variances, after comparing the variances by the *F* test, whereas that of the median was examined by two-sided Mann-Whitney's *U* test. Statistical significance of the frequency was analyzed by two-sided Fisher's exact probability test, and that of the correlation was analyzed by two-sided Pearson's correlation coefficient after confirming the normality of the variables. All the statistical analyses were performed with SPSS 15.0 (SPSS, Chicago, IL, USA).

Fig. 1 Methylation analysis using leukocyte and placental genomic DNA. **a** The regional physical map of the two imprinted domains on human chromosome 11p15.5. Paternally expressed genes are shown in blue, maternally expressed genes in red, and the DMRs in green. The stippled ellipse indicates the enhancer for *IGF2* and *H19*. For the *H19*-DMR, a 317-bp region harboring 23 CpG dinucleotides, methylated allele-specific *Bsa*BI and *Mwo*I restriction sites, and the T/G SNP (*rs2251375*; gray boxes) was studied for leukocyte genomic DNA. The cytosine residues at the CpG dinucleotides are usually methylated after paternal transmission (filled circles) and unmethylated after maternal transmission (open circles); after bisulfite treatment, this region is digested with *Bsa*BI when the cytosine at the 6th CpG dinucleotide (indicated with a yellow rectangle) is methylated and with *Mwo*I when the two cytosines at the ninth and the 11th CpG dinucleotides (indicated with orange rectangles) are methylated. A short 189-bp region was analyzed for placental genomic DNA. For the KvDMR1, a 326-bp region harboring 24 CpG dinucleotides and methylated allele-specific *Hpy*188I and *Eci*I restriction sites was examined for leukocyte genomic DNA. The cytosine residues at the CpG dinucleotides are usually unmethylated after paternal transmission (open circles) and methylated after maternal transmission (filled circles); after bisulfite treatment, this region is digested with *Hpy*188I when the cytosine at the fifth CpG dinucleotide (indicated with a light green rectangle) is methylated and with *Eci*I when the cytosine at the 22nd CpG dinucleotide (indicated with a light blue rectangle) is methylated. **b** Representative results of the Bio-COBRA using leukocyte genomic DNA (U: unmethylated clone specific bands; M: methylated clone specific bands; and BWS: Beckwith-Wiedemann syndrome patient with upd(11p15)pat) and the histograms showing the distribution of the methylation indices (the horizontal axis: the methylation index with an interval of 2.5%; and the vertical axis: the patient number; the mean values of two independent experiments are utilized for cases 1–60). For the *H19*-DMR shown on the left side, U is predominant in cases 1 and 2, both U and M are found in cases 21 and 22 as well as in a control subject, and M is predominant in the BWS patient. For the KvDMR1 shown on the right side, both U and M are found in cases 1, 2, 21, and 22 as well as in a control subject, and U is predominant in the BWS case. **c** Bisulfite sequencing results of the *H19*-DMR in 20 cases with low methylation indices using leukocyte genomic DNA. For comparison, the data of cases 21 and 22 with normal methylation indices and of a control subject are also shown. Each line indicates a single clone, and each circle denotes a CpG dinucleotide; filled and open circles represent methylated and unmethylated cytosines, respectively. The T/G SNP (*rs2251375*) typing data are also indicated (P: patient; F: father; and M: mother). **d** Bisulfite sequencing results of the short *H19*-DMR using placental genomic DNA of five cases and a gestational age-matched control subject who is different from the control subject in **c**

Results

Methylation analysis and related studies using leukocytes

The methylation indices for the *H19*-DMR were below the normal range in 20 of the 60 SRS patients (cases 1–20; group 1) and within the normal range in the remaining 40 SRS patients (cases 21–60; group 2), whereas the indices for the KvDMR1 were similar between the SRS patients and the control subjects, without discernible hypermethylation in the SRS patients (Fig. 1b; the methylation index of each subject is shown in Supplementary Table 2, and the range and the median in groups 1 and 2 and the control subjects are

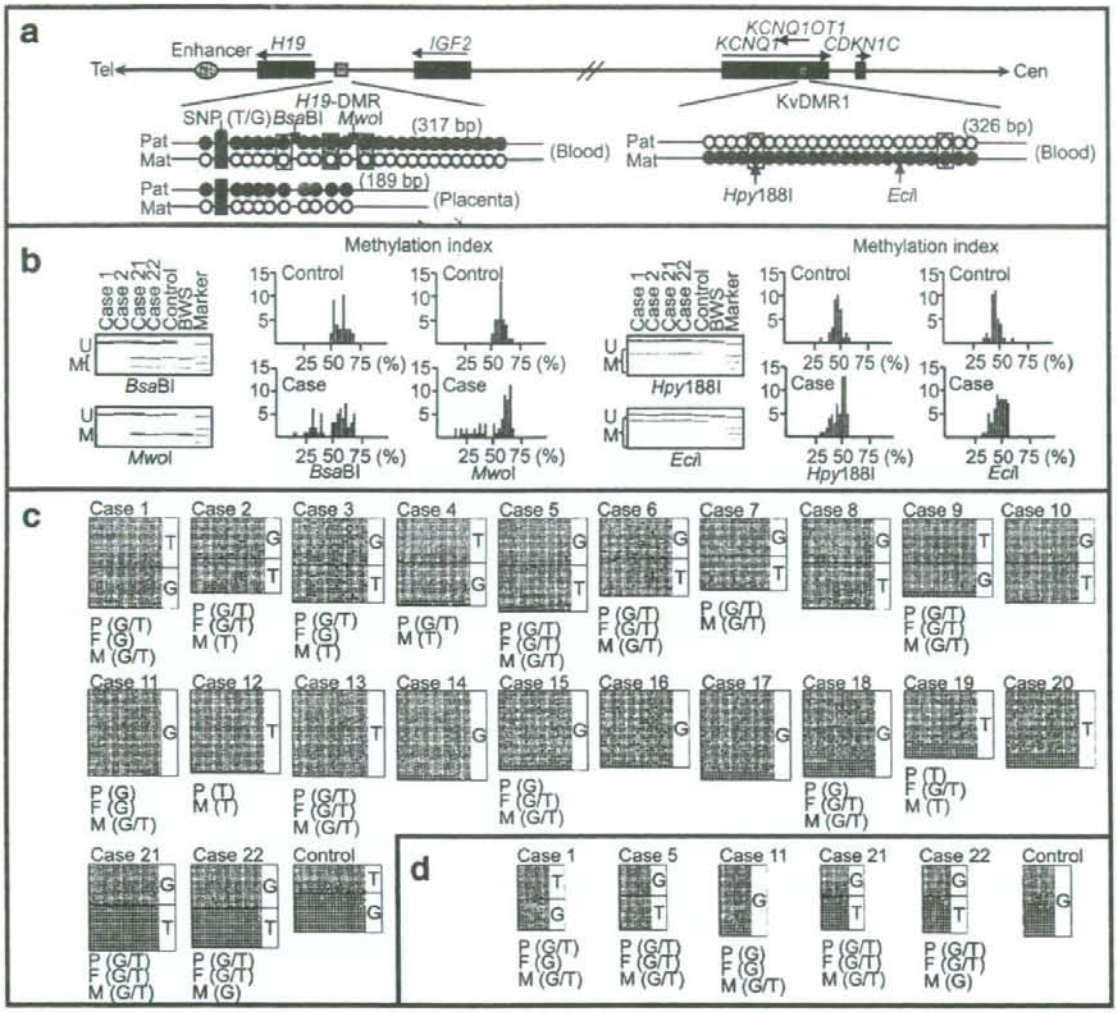

summarized in Supplementary Table 3). These results were reproduced in two independent experiments. Thus, we performed bisulfite sequencing, confirming hypomethylation of the *H19*-DMRs in cases 1–20 (Fig. 1c). In particular, the T/G SNP (*rs2251375*) typing within the amplified sequence showed heterozygosity for this SNP in cases 1–10, and genotyping analysis with available parental DNA samples demonstrated hypomethylation of paternally as well as maternally derived DMRs in cases 1–4. By contrast, similar analyses indicated parental origin dependent differentially methylated patterns in cases 21–60 of group 2 as well as in one normal subject.

In cases 1–20 of group 1, microsatellite analysis excluded maternal upd in 14 cases in whom parental DNA samples were available; in the remaining six cases in whom parental DNA samples were not available, microsatellite analysis identified two alleles for at least one locus, excluding maternal uniparental isodisomy for this region (Supplementary Table 4). Similarly, fluorescent in situ hybridization (FISH) analysis with an RP5-998N23 probe encompassing the *H19*-DMR showed two signals with a similar intensity in the 20 cases of group 1 (not shown). In addition, direct sequencing for seven putative CTCF binding sites at the *H19*-DMR did not show any substitution in the evolutionally conserved sequences [10], although two previously described SNPs (*rs10840167* and *rs10732516*) and two new SNPs were identified in the non-evolutionally conserved sequences at the sites 4 and 6 (Supplementary Table 5).

Methylation analysis using placentas

Methylation profiles of the *H19*-DMR were examined for formalin-treated and paraffin-embedded placental tissues of five SRS patients (cases 1, 5, and 11 in group 1 and cases 21 and 22 in group 2) and a nearly gestational age-matched control subject. Since the genomic DNA samples were rather fragmented because of the tissue treatment, we studied a short segment within the *H19*-DMR (Fig. 1a).

The methylation pattern was qualitatively similar to that identified in the leukocyte genomic DNA, and the *H19*-DMR was found to behave as the DMR in the placentas as well (Fig. 1d; see also Supplementary Fig. 1). In this regard, since a small number of maternal leukocytes would be present in the placental samples, this would have more or less influenced the methylation pattern. Indeed, the methylation indices for the *Bsa*BI site were somewhat high in cases 1, 5, and 11 in group 1, but not in cases 21 and 22 in group 2, as compared with those of leukocytes (Supplementary Table 2).

Expression studies using leukocytes and placentas

Expression analyses were performed for *IGF2* and *H19*, using the leukocyte and the placental samples of cases 1, 5, and 11 in group 1 and cases 21 and 22 in group 2. In addition, we also examined three control familial sample sets consisting of similarly treated placental tissue, umbilical cord blood cells, and parental blood cells.

For expression dosage, RT-PCR analysis indicated faint possible *IGF2* expression and slight *H19* expression after 35 PCR cycles in the leukocytes (not shown) and clear *IGF2* and *H19* expressions after 25–30 PCR cycles in the placentas (Fig. 2a). Notably, the *IGF2* expression level appeared to be decreased in the placentas of cases 1, 5, and 11 with epimutations and nearly normal in the placentas of cases 21 and 22 without epimutations, whereas *H19* expression level was apparently similar among the six placentas. While the precise quantification was difficult because of the poor RNA quality, similar results were reproduced in four independent experiments. Furthermore, the correct amplicon sizes produced by intron-spanning primer sets demonstrated the absence of genomic DNA contamination. In this regard, while a small number of maternal leukocytes may be present in the placental tissues, the influence would be negligible because of the faint *IGF2* and slight *H19* expressions in this cell type.

For expression pattern, genotyping for exonic SNPs revealed informative data in case 11 and in one control subject (Fig. 2b). In the leukocytes, although an electropherogram using cDNA was not obtained for *IGF2*, it was obtained for *H19*, indicating biallelic expression in case 11 and monoallelic maternal expression in the control subject. In the placentas, *IGF2* displayed monoallelic paternal expression, and *H19* showed monoallelic maternal expression in case 11 and the control subject. Notably, therefore, despite the *H19*-DMR being similarly hypomethylated in both the leukocytes and the placenta, *H19* of case 11 showed a different expression pattern between the leukocytes and the placenta.

Phenotypes of the patients

Body phenotypes are summarized in Table 1. Despite the gestational age being comparable between groups 1 and 2, birth length and weight were more severely compromised in group 1 than in group 2, and birth occipitofrontal head circumference (OFC) was better preserved in group 1 than in group 2. These auxological differences became non-significant in the postnatal life [in cases treated with growth hormone (GH), growth data before GH therapy were utilized], and comparison of the birth and the present auxological data revealed significant improvement in the body growth, but not in the OFC, in group 1, and no such

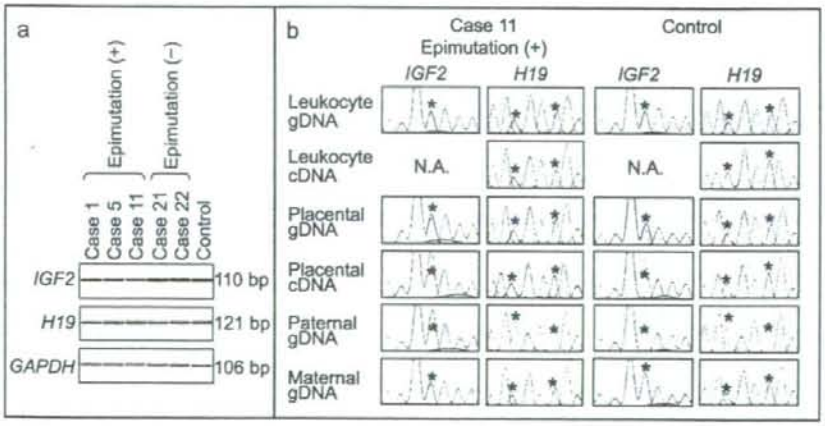

Fig. 2 Expression studies using leukocytes and placentas. **a** RT-PCR analysis (30 cycles) using formalin-treated and paraffin-embedded placental samples of case 1 (37 weeks of gestational age), case 2 (37 weeks), case 11 (35 weeks), case 21 (35 weeks), case 22 (34 weeks), and a normal individual (35 weeks). **b** Expression pattern analysis by genotyping of exonic SNPs (the A/G SNP *rs680* for *IGF2*; the G/A SNP *rs2839703* and the G/A SNP *rs2839704* for *H19*) in case 11 and a control subject. The three SNPs are marked with asterisks. N.A.: Not amplified; gDNA: genomic DNA

Table 1 Clinical features in the Silver-Russell syndrome patients examined in this study

	Group 1: Epimutation (+), n=20 (M/F=6:14)	Group 2: Epimutation (−), n=40 (M/F=25:15)	P value
Gestational age (weeks/days)	37:5 (28:4~41:0)	37:5 (32:0~41:4)	0.251
Birth length (SDS)[a]	−4.9±1.7	−3.1±1.4	<0.001
Birth weight (SDS)[a]	−3.5±0.9	−2.7±0.9	0.003
Birth OFC (SDS)[a]	−0.6±1.2	−1.9±1.1	0.003
Present age (years/months)	4.5 (1:3~30:6)	9:0 (0:1~18:6)	0.300
Present height (SDS)[b]	−3.4±1.8	−3.0±1.3	0.314
Present weight (SDS)[b]	−2.8±1.3	−2.2±0.8	0.094
Present OFC (SDS)[b]	−1.3±1.0	−2.0±1.1	0.191
Triangular face	100%	100%	1.000
Clinodactyly V	89.5%	85.2%	1.000
Relative macrocephaly	100%	69.6%	0.012
Ear anomalies	47.1%	29.2%	0.195
Body asymmetry	100%	30.0%	<0.001
Brachydactyly V	94.7%	70.4%	0.061
Mouth abnormalities	92.9%	27.3%	<0.001
Muscular hypotonia	69.2%	18.2%	0.004
Developmental delay	55.0%	38.5%	0.372
Irregular teeth	63.6%	38.1%	0.266
Simian crease	15.4%	14.3%	1.000
Syndactyly	11.1%	12.0%	1.000
Café au lait naevi	21.4%	13.0%	0.653
Precocious puberty	100%	36.4%	0.077
Genital abnormalities	37.5%	38.5%	1.000
Speech delay	23.5%	43.5%	0.315
Feeding difficulties	52.9%	48.0%	1.000
Serum IGF2 level (ng/mL)[c]	946.5 (694~1,158) (n=10)	1,070 (607~1,472) (n=5)	0.540
Paternal age at birth (years)	33 (19~52)	32 (25~45)	0.933
Maternal age at birth (years)	31.5 (19~39)	30 (24~39)	0.474
Mid-parental height (SDS)[b]	−0.3±0.7	−0.7±0.9	0.075

Significant difference was identified between the birth and present length/height SDSs (P=0.0074) and between the birth and present weight SDSs (P=0.0022), but not between the birth and present OFC SDSs (P=0.11) in group 1; in group 2, no statistical significance was identified between the birth and present length/height SDSs (P=0.78), between the birth and present weight SDSs (P=0.083), or between the birth and present OFC SDSs (P=0.96).

M Male, *F* female, *SDS* standard deviation score, *OFC* occipitofrontal head circumference, *IGF2* insulin-like growth factor 2

[a] Assessed by the gestational age- and sex-matched Japanese reference data from the Ministry of Health, Labor, and Welfare

[b] Assessed by the age- and sex-matched Japanese reference data from the Ministry of Health, Labor, and Welfare and from the Ministry of Education, Science, Sports and Culture

[c] Reference range: 400~1,100 ng/mL [5]

improvement in group 2 (Table 1, footnote). In addition, cases 17 and 18 with several methylated clones (Fig. 1c) had relatively well-preserved birth lengths or weights and spontaneously attained heights within the normal range (Supplementary Fig. 2); while cases 19 and 20 also had several methylated clones, case 19 was born at 28 weeks of gestation and was currently in her infancy, and case 20, though he had normal adult height at 20 years of age (−1.9 SD), had received GH and gonadal suppression therapy for a long term. Somatic features such as relative macrocephaly, body asymmetry, downward slanting corners of mouth, and muscular hypotonia were more frequent in group 1 than in group 2. The serum IGF2 value was normal to high in both groups. Furthermore, case 13 in group 1 was found to be born after intracytoplasmic sperm injection because of oligozoospermia. Parental ages were similar between the two groups, as were mid-parental heights.

Placental phenotypes

Placental phenotypes are summarized in Table 2. Placental hypoplasia was frequently identified in both groups and was more severe in group 1 than in group 2. In addition, oligohydramnios was also frequently detected in both groups with no significant difference. Histological examination revealed hypoplastic chorionic villi in cases 1, 5, and 11 of group 1 and in case 22 of group 2, and massive infarction and multiple syncytial knots in case 21 of group 2 (Fig. 3).

Table 2 Placental and amniotic fluid findings in this study

	Group 1: Epimutation (+), n=12 (M/F=5:7)	Group 2: Epimutation (−), n=10 (M/F=6:4)	P value
Placental weight (SDS)[a]	−1.78 (−2.38 to −0.78) −1.75±0.44	−1.20 (−1.66 to +0.98) Normality (−)[b]	0.004
Placental hypoplasia[a]			
<−2.0 SD	4/12	0/10	0.096
<−1.5 SD	10/12	2/10	0.008
<−1.0 SD	11/12	6/10	0.135
Oligohydramnios	7/11	6/14	0.428

M Male, *F* female, *SDS* standard deviation score
[a] Assessed by the gestational age-matched Japanese reference data for the placental weight [39]
[b] Placental size SDSs in group 2 did not follow the normal distribution.

Correlations studies between methylation index, body size, and placental weight

Correlation data in group 1 are shown in Table 3. The methylation index for the *H19*-DMR was positively correlated with the birth weight and length, the present weight and height, and the placental weight, but not with the birth OFC or the present OFC. Furthermore, the placental weight was positively correlated with the birth weight and length, but not with the birth OFC. Such positive correlations were not found in group 2. In addition, no significant correlations were identified between the methylation index for the KvDMR1 and the growth parameters in both groups 1 and 2.

Discussion

Molecular studies for leukocytes identified hypomethylation of the *H19*-DMR in one-third of the Japanese SRS patients and no hypermethylation of the KvDMR1. Although such hypomethylation in SRS patients could be caused by maternal upd involving the *H19*-DMR or by cryptic duplication involving the maternally inherited *H19*-DMR (cryptic deletion affecting the paternally inherited *H19*-DMR, though it results in a hypomethylated *H19*-DMR, would permit a normal phenotype) [13, 27, 28], this possibility is argued against by the microsatellite and FISH analyses. While the frequency of epimutations tended to be lower than that of the previous European studies [2–6], this

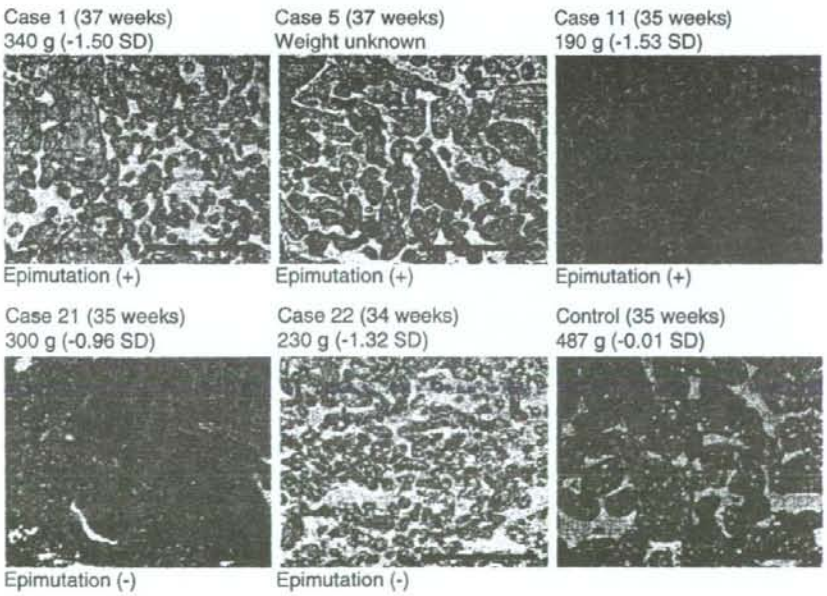

Fig. 3 Histological findings of the placentas (hematoxylin–eosin staining). The placental weight is described for each placenta, together with the SD score assessed by the gestational age-matched placental reference data [39]. The bars represent 100 μm

Table 3 Correlation analyses in patients with epimutations

	Restriction enzymes	*r*	*P* value
Methylation index (%)[a] vs.			
Birth weight (SDS)	*Bsa*BI	0.50	0.026
	*Mwo*I	0.50	0.024
Birth length (SDS)	*Bsa*BI	0.46	0.031
	*Mwo*I	0.49	0.022
Birth OFC (SDS)	*Bsa*BI	−0.04	0.903
	*Mwo*I	−0.14	0.629
Present weight (SDS)	*Bsa*BI	0.47	0.042
	*Mwo*I	0.58	0.010
Present height (SDS)	*Bsa*BI	0.53	0.019
	*Mwo*I	0.49	0.035
Present OFC (SDS)	*Bsa*BI	0.02	0.968
	*Mwo*I	−0.37	0.369
Placental weight (SDS)	*Bsa*BI	0.53	0.038
	*Mwo*I	0.59	0.021
Placental weight (SDS) vs.			
Birth weight (SDS)		0.83	0.001
Birth length (SDS)		0.61	0.036
Birth OFC (SDS)		0.16	0.612

SDS Standard deviation score, *OFC* occipitofrontal head circumference, *r* correlation coefficient

[a] The mean value of two independent experiments is utilized for each case.

may be due to the difference in the ethnic groups or in the selection criteria (several patients with postnatal catch-up growth were included in the present study). In addition, while the methylation indices for the *H19*-DMR were skewed to the hypermethylation side, such skewing appears to be a fairly common phenomenon probably caused by different PCR amplification efficiencies between cytosine- and thymine-rich DNA sequences after bisulfite treatment [26, 29].

The placental molecular studies, in conjunction with leukocyte expression analyses, provide several important findings. First, since the epimutation of the *H19*-DMR reduced *IGF2* expression in the placentas of three patients, it is likely that placental *IGF2* expression is primarily dependent on the methylation status of the *H19*-DMR. Second, the biparental expression of *H19* in the epimutation-positive leukocytes is consistent with maternalization of the paternally derived *IGF2–H19* imprinted domain. Third, the monoallelic maternal expression of *H19* implies that the placental *H19* expression is also regulated by some mechanism(s), other than the methylation pattern of the *H19*-DMR, such as the control of chromatin conformation [15, 22, 23], and explains why the placental *H19* expression level was apparently similar irrespective of the presence or absence of epimutations. However, since informative *H19* expression patterns were shown only in a single case (case 11), further studies are necessary to have a definitive conclusion.

The clinical phenotypes of the patients are primarily consistent with those reported previously [5, 6]. Patients with epimutations had typical SRS features and normal to high serum IGF2 levels. In this context, *IGF2* shows a biallelic expression pattern in the human fetal brain [30], and while the biparental *IGF2* expression becomes region-specific in the adult brain [31], brain development is mostly completed during the fetal period. This would explain why the birth as well as the present OFC was well preserved in group 1. Similarly, the serum IGF2 levels would be compatible with those being primarily derived from the liver in which *IGF2* is expressed biallelically from late gestation depending on the liver specific promoter [32].

Phenotypic assessment of the placentas has also revealed characteristic features. The small placentas with hypoplastic chorionic villi in group 1 would be ascribed to the reduced *IGF2* expression in the placenta. Indeed, *IGF2* is expressed in chorionic villi [33], and mice deficient for the placental specific *Igf2* promoter have small placentas with reduced diffusional permeability suggestive of hypoplastic chorionic villi [34]. Furthermore, the small placenta with hypoplastic chorionic villi of case 22 in group 2 would suggest the presence of a hitherto unknown (epi)genetic factor(s) leading to SRS, whereas the small placenta with obvious infarction of case 21 in group 2 would imply the relevance of an environmental factor(s) affecting placental function to the SRS phenotypes, especially the growth failure. In addition, the frequent occurrence of oligohydramnios would reflect placental dysfunction in both groups.

The placental hypoplasia would have affected the prenatal growth. Since the postnatal body growth was improved as compared with the prenatal body growth in group 1, this implies that the body growth in epimutation-positive SRS patients is severely compromised during the fetal life because of the effects of both intrinsic defects and placental abnormalities but is somewhat improved after birth because of the effects of intrinsic defects alone. In support of this notion, mice deficient for the placental specific *Igf2* promoter exhibit prenatal growth failure and postnatal catch-up growth [35].

Correlation analyses would suggest that *IGF2* expression level, as reflected by the methylation index of the *H19*-DMR, plays a positive role in the determination of body and placental growth in patients with epimutations. In this context, the positive correlation between placental weight and the birth length and weight would be mediated by the *IGF2* expression level, and the lack of correlation between the methylation index and the OFC would be compatible with the aforementioned brain *IGF2* expression pattern [30, 31]. Furthermore, since the *IGF2* expression level is variable and not correlated with birth size (weight and OFC) or placental weight in normal term placentas [36], it is likely that the *IGF2* expression level constitutes a relatively

major factor for body and placental growth in patients with epimutations as the primary disease-causing abnormality, but not in other individuals. Consistent with this, there were no positive correlations between the *H19*-DMR methylation index and growth parameters in group 2. One may argue that the methylation index also reflects the expression level of *H19*. However, this would not have a major clinical effect because the primary function of *H19* in the bodies appears to be tumor suppression [37, 38]. In addition, since *H19* showed monoallelic maternal expression with apparently normal expression level in the epimutation-positive placenta, this would argue against the relevance of *H19* to placental phenotype.

In summary, the present study provides useful information for the definition of molecular and clinical findings and their correlations in bodies and placentas of epimutation-positive and epimutation-negative SRS patients. Further studies, especially those for placentas, will permit a better characterization of SRS.

Acknowledgments We would like to thank all the patients and their family members who participated in this study. We are also grateful to Drs. T. Tanaka, Z. Kizaki, S. Omori, M. Sugita, D. Ariyasu, M. Izawa, Y. Fujimoto, A. Shiokawa, K. Taniguchi, S. Matsubayashi, K. Satsuka, Y. Muramatsu, N. Amano, H. Kabata, and S. Ishii for sample collection and phenotypic assessment, and Drs. K. Hata and K. Nakabayashi for fruitful discussion. This work was supported by Grants for Child Health and Development (20C-2) and for Research on Children and Families (H18-005) from the Ministry of Health, Labor, and Welfare, and by Grants-in-Aid for Scientific Research (Priority Areas: 16086215; category B: 19390290) and Grant-in-Aid for Young Scientists (B) (19790752) from the Ministry of Education, Culture, Sports, Science and Technology, Japan.

References

1. Hitchins MP, Stanier P, Preece MA, Moore GE (2001) Silver-Russell syndrome: a dissection of the genetic aetiology and candidate chromosomal regions. J Med Genet 38:810–819
2. Gicquel C, Rossignol S, Cabrol S, Houang M, Steunou V, Barbu V, Danton F, Thibaud N, Le Merrer M, Burglen L, Bertrand AM, Netchine I, Le Bouc Y (2005) Epimutation of the telomeric imprinting center region on chromosome 11p15 in Silver-Russell syndrome. Nat Genet 37:1003–1007
3. Bliek J, Terhal P, van den Bogaard MJ, Maas S, Hamel B, Salieb-Beugelaar G, Simon M, Letteboer T, van der Smagt J, Kroes H, Mannens M (2006) Hypomethylation of the H19 gene causes not only Silver-Russell syndrome (SRS) but also isolated asymmetry or an SRS-like phenotype. Am J Hum Genet 78:604–614
4. Eggermann T, Schonherr N, Meyer E, Obermann C, Mavany M, Eggermann K, Ranke MB, Wollmann HA (2006) Epigenetic mutations in 11p15 in Silver-Russell syndrome are restricted to the telomeric imprinting domain. J Med Genet 43:615–616
5. Netchine I, Rossignol S, Dufourg MN, Azzi S, Rousseau A, Perin L, Houang M, Steunou V, Esteva B, Thibaud N, Demay MC, Danton F, Petriczko E, Bertrand AM, Heinrichs C, Carel JC, Loeuille GA, Pinto G, Jacquemont ML, Gicquel C, Cabrol S, Le Bouc Y (2007) 11p15 imprinting center region 1 loss of methylation is a common and specific cause of typical Russell-Silver syndrome: clinical scoring system and epigenetic–phenotypic correlations. J Clin Endocrinol Metab 92:3148–3154
6. Binder G, Seidel AK, Martin DD, Schweizer R, Schwarze CP, Wollmann HA, Eggermann T, Ranke MB (2008) The endocrine phenotype in Silver-Russell syndrome is defined by the underlying epigenetic alteration. J Clin Endocrinol Metab 93:1402–1407
7. Leighton PA, Saam JR, Ingram RS, Stewart CL, Tilghman SM (1995) An enhancer deletion affects both H19 and Igf2 expression. Genes Dev 9:2079–2089
8. Leighton PA, Ingram RS, Eggenschwiler J, Efstratiadis A, Tilghman SM (1995) Disruption of imprinting caused by deletion of the H19 gene region in mice. Nature 375:34–39
9. Thorvaldsen JL, Duran KL, Bartolomei MS (1998) Deletion of the H19 differentially methylated domain results in loss of imprinted expression of H19 and Igf2. Genes Dev 12:3693–3702
10. Bell AC, Felsenfeld G (2000) Methylation of a CTCF-dependent boundary controls imprinted expression of the Igf2 gene. Nature 405:482–485
11. Hark AT, Schoenherr CJ, Katz DJ, Ingram RS, Levorse JM, Tilghman SM (2000) CTCF mediates methylation-sensitive enhancer-blocking activity at the H19/Igf2 locus. Nature 405:486–489
12. Binder G, Seidel AK, Weber K, Haase M, Wollmann HA, Ranke MB, Eggermann T (2006) IGF-II serum levels are normal in children with Silver-Russell syndrome who frequently carry epimutations at the IGF2 locus. J Clin Endocrinol Metab 91:4709–4712
13. Fisher AM, Thomas NS, Cockwell A, Stecko O, Kerr B, Temple IK, Clayton P (2002) Duplications of chromosome 11p15 of maternal origin result in a phenotype that includes growth retardation. Hum Genet 111:290–296
14. Coan PM, Burton GJ, Ferguson-Smith AC (2005) Imprinted genes in the placenta—a review. Placenta 26(Suppl A):S10–20
15. Wagschal A, Feil R (2006) Genomic imprinting in the placenta. Cytogenet Genome Res 113:90–98
16. Yamazawa K, Kagami M, Ogawa M, Horikawa R, Ogata T (2008) Placental hypoplasia in maternal uniparental disomy for chromosome 7. Am J Med Genet Part A 146A:514–516
17. Robinson WP, Slee J, Smith N, Murch A, Watson SK, Lam WL, McFadden DE (2007) Placental mesenchymal dysplasia associated with fetal overgrowth and mosaic deletion of the maternal copy of 11p15.5. Am J Med Genet Part A 143A:1752–1759
18. Kagami M, Sekita Y, Nishimura G, Irie M, Kato F, Okada M, Yamamori S, Kishimoto H, Nakayama M, Tanaka Y, Matsuoka K, Takahashi T, Noguchi M, Tanaka Y, Masumoto K, Utsunomiya T, Kouzan H, Komatsu Y, Ohashi H, Kurosawa K, Kosaki K, Ferguson-Smith AC, Ishino F, Ogata T (2008) Deletions and epimutations affecting the human 14q32.2 imprinted region in individuals with paternal and maternal upd(14)-like phenotypes. Nat Genet 40:237–242
19. Fowden AL, Sibley C, Reik W, Constancia M (2006) Imprinted genes, placental development and fetal growth. Horm Res 65 (Suppl 3):50–58
20. Hurst LD, McVean GT (1997) Growth effects of uniparental disomies and the conflict theory of genomic imprinting. Trends Genet 13:436–443
21. Eggermann T, Zerres K, Eggermann K, Moore G, Wollmann HA (2002) Uniparental disomy: clinical indications for testing in growth retardation. Eur J Pediatr 161:305–312
22. Monk D, Arnaud P, Apostolidou S, Hills FA, Kelsey G, Stanier P, Feil R, Moore GE (2006) Limited evolutionary conservation of imprinting in the human placenta. Proc Natl Acad Sci U S A 103:6623–6628
23. Lin SP, Coan P, da Rocha ST, Seitz H, Cavaille J, Teng PW, Takada S, Ferguson-Smith AC (2007) Differential regulation of imprinting in the murine embryo and placenta by the Dlk1-Dio3 imprinting control region. Development 134:417–426

24. Kotzot D (2004) Maternal uniparental disomy 14 dissection of the phenotype with respect to rare autosomal recessively inherited traits, trisomy mosaicism, and genomic imprinting. Ann Genet 47:251–260
25. Vu TH, Li T, Nguyen D, Nguyen BT, Yao XM, Hu JF, Hoffman AR (2000) Symmetric and asymmetric DNA methylation in the human IGF2–H19 imprinted region. Genomics 64:132–143
26. Brena RM, Auer H, Kornacker K, Hackanson B, Raval A, Byrd JC, Plass C (2006) Accurate quantification of DNA methylation using combined bisulfite restriction analysis coupled with the Agilent 2100 Bioanalyzer platform. Nucleic Acids Res 34:e17
27. Eggermann T, Meyer E, Obermann C, Heil I, Schuler H, Ranke MB, Eggermann K, Wollmann HA (2005) Is maternal duplication of 11p15 associated with Silver-Russell syndrome? J Med Genet 42:e26
28. Sparago A, Cerrato F, Vernucci M, Ferrero GB, Silengo MC, Riccio A (2004) Microdeletions in the human H19 DMR result in loss of IGF2 imprinting and Beckwith-Wiedemann syndrome. Nat Genet 36:958–960
29. Warnecke PM, Stirzaker C, Melki JR, Millar DS, Paul CL, Clark SJ (1997) Detection and measurement of PCR bias in quantitative methylation analysis of bisulphite-treated DNA. Nucleic Acids Res 25:4422–4426
30. Ulaner GA, Yang Y, Hu JF, Li T, Vu TH, Hoffman AR (2003) CTCF binding at the insulin-like growth factor-II (IGF2)/H19 imprinting control region is insufficient to regulate IGF2/H19 expression in human tissues. Endocrinology 144:4420–4426
31. Pham NV, Nguyen MT, Hu JF, Vu TH, Hoffman AR (1998) Dissociation of IGF2 and H19 imprinting in human brain. Brain Res 810:1–8
32. Ekstrom TJ, Cui H, Li X, Ohlsson R (1995) Promoter-specific IGF2 imprinting status and its plasticity during human liver development. Development 121:309–316
33. Han VK, Carter AM (2000) Spatial and temporal patterns of expression of messenger RNA for insulin-like growth factors and their binding proteins in the placenta of man and laboratory animals. Placenta 21:289–305
34. Sibley CP, Coan PM, Ferguson-Smith AC, Dean W, Hughes J, Smith P, Reik W, Burton GJ, Fowden AL, Constancia M (2004) Placental-specific insulin-like growth factor 2 (Igf2) regulates the diffusional exchange characteristics of the mouse placenta. Proc Natl Acad Sci U S A 101:8204–8208
35. Constancia M, Hemberger M, Hughes J, Dean W, Ferguson-Smith A, Fundele R, Stewart F, Kelsey G, Fowden A, Sibley C, Reik W (2002) Placental-specific IGF-II is a major modulator of placental and fetal growth. Nature 417:945–948
36. Apostolidou S, Abu-Amero S, O'Donoghue K, Frost J, Olafsdottir O, Chavele KM, Whittaker JC, Loughna P, Stanier P, Moore GE (2007) Elevated placental expression of the imprinted PHLDA2 gene is associated with low birth weight. J Mol Med 85:379–387
37. Hao Y, Crenshaw T, Moulton T, Newcomb E, Tycko B (1993) Tumour-suppressor activity of H19 RNA. Nature 365:764–767
38. Juan V, Crain C, Wilson C (2000) Evidence for evolutionarily conserved secondary structure in the H19 tumor suppressor RNA. Nucleic Acids Res 28:1221–1227
39. Nakayama M (2002) Placental Pathology. Igaku Shoin, Tokyo (in Japanese)

[Epigenetics 3:4, 181-187; July/August 2008]; ©2008 Landes Bioscience

Point of View

Molecular mechanisms regulating phenotypic outcome in paternal and maternal uniparental disomy for chromosome 14

Tsutomu Ogata,[1,*] Masayo Kagami[1] and Anne C. Ferguson-Smith[2]

[1]Department of Endocrinology and Metabolism; National Research Institute for Child Health and Development; Tokyo, Japan; [2]Department of Physiology; Development and Neuroscience; University of Cambridge; Cambridge UK

Key words: upd(14)pat, upd(14)mat, phenotype, IG-DMR, DLK1, RTL1

Human chromosome 14q32.2 carries a cluster of imprinted genes including paternally expressed genes (*PEGs*) such as *DLK1* and *RTL1*, and maternally expressed genes (*MEGs*) such as *GTL2* (alias, *MEG3*), *RTL1as* (*RTL1* antisense) and *MEG8*. Consistent with this, paternal and maternal uniparental disomies for chromosome 14 (upd(14)pat and upd(14)mat) cause distinct phenotypes. In this report, we review the current knowledge about the underlying factors for the development of clinical features in upd(14)pat and upd(14)mat. The data available suggest that the *DLK1-GTL2* IG-DMR functions as a regulator for the maternally inherited imprinted region, and that excessive *RTL1* expression and decreased *DLK1* and *RTL1* expression play a major role in the development of upd(14)pat-like and upd(14)mat-like phenotypes, respectively.

Human chromosome 14q32.2 carries a cluster of imprinted genes including paternally expressed genes (*PEGs*) such as *DLK1* and *RTL1*, and maternally expressed genes (*MEGs*) such as *GTL2* (alias, *MEG3*), *RTL1as* (*RTL1* antisense) and *MEG8* (Fig. 1).[1,2] Although it remains to be clarified whether *DIO3* is a *PEG*, mouse *Dio3* is known to be preferentially but not exclusively expressed from paternally derived chromosome.[3] The parent-of-origin specific monoallelic expression patterns are tightly related to the methylation status of differentially methylated regions (DMRs).[4] For the 14q32.2 imprinted region, the *DLK1-GTL2* intergenic DMR (IG-DMR) and the *GTL2*-DMR are extensively hypermethylated after paternal transmission and grossly hypomethylated after maternal transmission.[5-8]

Consistent with these findings, both paternal and maternal uniparental disomies for chromosome 14 (upd(14)pat and upd(14)mat) cause distinct phenotypes. Upd(14)pat results in a unique phenotype characterized by facial abnormality, small bell-shaped thorax, abdominal wall defects and polyhydramnios.[8] In particular, the bell-shaped thorax is pathognomonic and may be lethal or require long-term mechanical ventilation. Upd(14)mat leads to clinically discernible features such as pre- and postnatal growth failure, hypotonia, mild facial abnormalities, small hands and early onset of puberty.[8,9] The phenotypic spectrum in upd(14)mat is wide and ranges from nearly normal phenotype to a severe phenotype reminiscent to that of Prader-Willi syndrome.[10,11] Furthermore, in agreement with the pivotal role of imprinted genes in placental growth and development,[12,13] upd(14)pat is associated with placentomegaly,[8,14] while placental size has not been examined in upd(14)mat.

Such phenotypic development is ascribed to perturbed expression of imprinted genes, i.e., increased expression of *PEGs* and absent expression of *MEGs* in upd(14)pat and increased expression of *MEGs* and absent expression of *PEGs* in upd(14)mat. In this regard, we have recently proposed the major factors for the development of upd(14)pat/mat phenotypes, on the basis of (epi)genotype-phenotypes correlations in a total of 12 patients with microdeletions and epimutations affecting the imprinted region as well as the mouse data available. Here, we first summarize the current knowledge about the mouse homologous region and subsequently explain the underlying mechanisms leading to the development of human upd(14)pat/mat phenotypes. We also refer to the placental data in comparison with the body data.

Summary of Mouse Data

Uniparental disomy for chromosome 12. The human 14q32.2 imprinted region is highly conserved on the distal part of the mouse chromosome 12.[15] The imprinted genes on the distal chromosome 12 show monoallelic expression in both the normal embryos and placentas.[12,16] Thus, paternal uniparental disomy for chromosome 12 [PatDi(12)] results in a distinct clinical phenotype that includes prenatal lethality, cartilage defects, abdominal distension and placentomegaly, whereas MatDi(12) leads to characteristic phenotype such as perinatal lethality, growth failure (~60%), and placental hypoplasia.[17] Although lethality is more obvious in the affected mice, and rib anomaly in paternal disomies is more evident in the affected humans, the considerable degree of analogy in the clinical features suggest the involvement of similar (epi)genetic mechanisms in both human and mouse disomies for the conserved imprinted region.

Targeted deletion of the IG-DMR (ΔIG-DMR). This deletion experiment has shown that the germ-line derived IG-DMR functions as a cis-acting regulator for the imprinted region of maternal origin in the embryo.[6,18] Namely, ΔIG-DMR causes paternalization of a maternally derived imprinted region and a unique phenotype

*Correspondence to: Tsutomu Ogata; National Research Institute for Child Health and Development; Department of Endocrinology and Metabolism; 2-10-1 Ohkura; Setagaya; Tokyo, Kanto 157-8535 Japan; Email: tomogata@nch.go.jp

Submitted: 01/30/08; Accepted: 07/02/08

Previously published online as an *Epigenetics* E-publication: http://www.landesbioscience.com/journals/epigenetics/article/6550

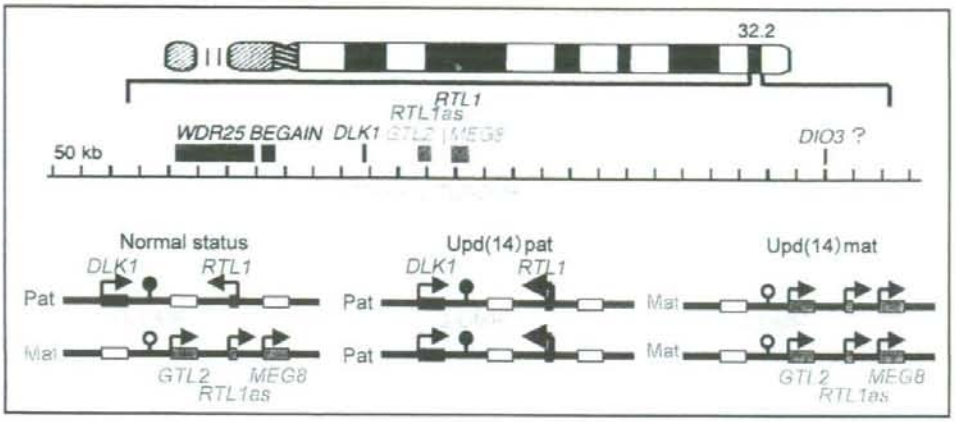

Figure 1. The human chromosome 14q32.2 imprinted region and the expression patterns of the imprinted genes. *PEGs* are shown in blue and *MEGs* in red; it remains to be clarified whether *DIO3* is a *PEG*.[3] *WDR25* and *BEGAIN* appear biparentally expressed genes. The IG-DMR and the GTL2-DMR are depicted in green. In the normal status, all the *PEGs* and *MEGs* show monoallelic expression patterns, in association with the parental origin specific methylation patterns of the DMRs. In upd(14)pat, *PEGs* are expressed from both chromosomes, with severely increased *RTL1* expression because of the absence of the functional *RTL1as*. In upd(14)mat, *MEGs* are expressed from both chromosomes.

comparable to that of PatDi(12) in embryos, with ~4.5 times of *Rtl1* expression and ~2 times of *Dlk1* and *Dio3* expression as well as nearly absent expression of *Megs*.[6,16,17] The marked *Rtl1* overexpression is ascribed to a synergic effect between activation of the usually silent maternally derived *Rtl1* and loss of functional *Rtl1as* which acts as a repressor for *Rtl1*.[6,19] This negative regulation occurs because *Rtl1as* is the primary transcript for seven miRNAs which, when processed, target the paternally expressed *Rtl1* mRNA in an RNAi-dependent manner hence reducing its levels.[6,20] The doubled *Dlk1* and *Dio3* expression is simply due to the activation of *Pegs* of maternal origin.[6] The absent *Megs* expression is associated with hypermethylation of the *Gtl2*-DMR,[6] consistent with the notion that methylation pattern of the *Gtl2*-DMR is established after fertilization depending on the methylation of the IG-DMR (the *Gtl2*-DMR can stay hypomethylated only when the IG-DMR is hypomethylated).[18] By contrast, the ΔIG-DMR has no imprinting or clinical effect after paternal transmission.[6]

Knockout mouse experiments. Knockout mouse experiments have successfully been performed for *Dlk1*, *Rtl1*/*Rtl1as* and *Dio3*. The *Dlk1* mutation causes several upd(14)mat-like features such as pre- and postnatal growth deficiency (~80%), obesity, and facial abnormalities only after paternal transmission.[21] The paternally inherited *Rtl1* deletion results in mild growth deficiency (~80%),[22] and the maternally derived *Rtl1as* deletion leads to placentomegaly and dilated fetal capillaries in the labyrinth zone in association with 2.5–3.0 times of *Rtl1* expression.[22] *Dio3* knockout mice show reduced enzyme activities and some phenotypic effects after paternal transmission.[23] Furthermore, *Gtl2*^{lacZ} mice with dysregulated imprinting caused by a transgene insertion have a normal phenotype with at least 60–80% reduction of all the *Megs*.[24]

Placental analysis. Placental analyses have revealed different expression patterns and phenotypes between the PatDi(12) mice and the ΔIG-DMR mice. While mice with PatDi(12) have placentomegaly,[17] those with maternally derived ΔIG-DMR have normal placentas with mildly increased *Pegs* expression and considerably preserved *Megs* expression.[16] In addition, while the IG-DMR methylation pattern is comparable between the normal mouse embryo and placenta, the *Gtl2*-DMR in the embryo does not similarly resemble a DMR in the placenta, with both alleles showing partial methylation with the difference between them being only ~25%.[16] These findings suggest subtle differences in imprinting control and resultant phenotypic consequences between the embryos and placentas with ΔIG-DMR.

Summary of Human Data

Identification of the IG-DMR and the *GTL2*-DMR. We and other investigators have identified the human IG-DMR.[5,6,8] In particular, we found two regions with the property of the IG-DMR, designated CG4 and CG6. We have also identified the human *GTL2*-DMR designated CG7. Although the *GTL2*-DMR has been reported previously,[7] CG7 was confirmed to be the *GTL2*-DMR by bisulfite sequencing.[8]

(Ei)genotype-phenotype correlations and proposed hypothesis. To date, eight non-disomic patients with upd(14)pat-like phenotype and nine non-disomic patients with upd(14)mat-like phenotype have been reported in the literature.[8,25-27] Phenotype, actual gene dosage, and predicted expressed gene dosage in such patients are summarized in Tables 1 and 2, together with those in upd(14)pat/mat patients.

On the basis of (epi)genotype-phenotype in such patients, we have proposed that the IG-DMR exerts an important regulatory function for the maternally inherited imprinted region, and that excessive *RTL1* expression and decreased *DLK1* and *RTL1* expression play a major role in the development of upd(14)pat-like and upd(14)mat-like phenotypes, respectively. This hypothesis assumes that the functions of the IG-DMR and the imprinted genes within this domain are primarily similar between the human and the mouse.[8]

We present here how this hypothesis can explain the development of upd(14)pat/mat-like phenotypes in non-disomic patients. We do not refer to *DIO3* and *MEGs* other than *RTL1as*; although the relevance of *DIO3* and the total absence of *MEGs* still remains tenable at this time, upd(14)pat/mat patients are apparently free from thyroid

Table 1 (Epi)genotype-phenotype correlations in patients with upd(14)pat-like phenotypes

	Upd(14)pat-like phenotype positive patients					Upd(14)pat patients	Normal subjects
	Deletions				Epimutations		
	Cases 1 and 2 ref. 8	Case 3 ref. 8	Case 4 ref. 8	Case 5 ref. 8	Cases 6–8 ref. 8	(n = 17) ref. 8, 14	
Phenotype							
Characteristic face	+	+	+	+	3/3	100%	-
Bell-shaped thorax	+	+[a]	+[a]	+[a]	3/3	100%	-
Abdominal wall defects	+	±	±	±	3/3	100%	-
Polyhydramnios	+	+[b]	+[b]	±	3/3	100%	-
Placentomegaly	+	+	+	±	3/3	100%	-
Actual gene dosage							
DLK1	1	1	2	1	2	2	2
GTL2	1	1	1	1	2	2	2
RTL1	2	1	1	1	2	2	2
RTL1as	2	1	1	1	2	2	2
MEG8	2	1	1	1	2	2	2
DIO3	2	2	2	1	2	2	2
Predicted expressed gene dosage[c]							
DLK1	1	1	2	1	2	2	1
GTL2	0	0	0	0	0	0	1
RTL1	~4.5	2–2.5	2–2.5	2–2.5	~4.5	~4.5	1
RTL1as	0	0	0	0	0	0	1
MEG8	0	0	0	0	0	0	1
DIO3	2	2	2	1	2	2	1

[a]The period of mechanical ventilation was relatively short. [b]Amniocentesis was required at the relatively late gestational age. [c]Primarily based on the mouse data of targeted IG-DMR deletion,[6] *Rtl1/Rtl1as* knockout,[22] and *Rtl1-Rtl1as* interaction.[19]

dysfunction, despite the primary function of *DIO3* being thyroid hormone metabolism,[3] and biological functions remains totally unknown for *MEGs* other than *RTL1as*.

Familial microdeletions (Family A). (Fig. 2) This unique three-generation family contains two sibs (III-1 and III-3) with typical upd(14)pat phenotype and the mother (II-2) and the maternal grandfather (I-3) with upd(14)mat-like phenotype including mild short stature (-2.2 SD in the mother and -2.9 SD in the grandfather)[8] (III-1 and III-3 correspond to cases 1 and 2 in Table 1, and , II-2 and I-3 correspond to cases 9 and 10 in Table 2). Methylation analysis showed hypermethylated DMRs in case III-3 and hypomethylated DMRs in cases II-2 and I-3. Deletion analysis revealed a ~109 kb deletion involving *DLK1*, the IG-DMR, the *GTL2*-DMR, and *GTL2* in cases with upd(14)pat/mat-like phenotypes. Thus, the deletion has caused typical upd(14)pat phenotype after maternal transmission and upd(14)mat-like phenotype after paternal transmission.

The results are well explained by the above notion. In the two sibs (III-1 and III-3) with typical upd(14)pat phenotype, since the loss of IG-DMR is derived from the mother, this would have caused paternalization of the imprinted domain, resulting in the expression of *PEGs* rather than *MEGs* from both chromosomes. However, since *DLK1* is deleted from the maternally inherited chromosome, *DLK1* should be present in a single active copy, as in normal individuals. By contrast, since *RTL1* is present in two copies in the absence of functional *RTL1as*, the expression dosage of *RTL1* should be increased markedly (4–5 times), as in upd(14)pat patients. Thus, it is likely that severely increased *RTL1* dosage plays a critical role in the development of the typical upd(14)pat phenotype.

In the mother (II-2) and the maternal grandfather (I-3) with upd(14)mat-like phenotype, since the loss of IG-DMR is of paternal origin, this would have no effect on the imprinting status. Thus, the upd(14)mat-like phenotype would simply be ascribed to the loss of *DLK1* from the paternally derived chromosome.

Familial microdeletions (family B). (Fig. 3) This two-generation family contains the daughter (III-1) with a relatively mild upd(14) pat-like phenotype in terms of the duration of respiratory defects, abdominal defects, and the degree of polyhydramnios, and the mother (II-2) with upd(14)mat-like phenotype including severe short stature (-4.4 SD)[8] (III-1 corresponds to case 3 in Table 1, and II-2 corresponds to case 11 in Table 2). Methylation analysis showed hypermethylated DMRs in case III-1 and hypomethylated DMRs in case II-2. Deletion analysis revealed a ~411 kb deletion involving *WDR25*, *BEGAIN*, *DLK1*, the IG-DMR, the *GTL2*-DMR, *GTL2*, *RTL1*, *RTL1as* and *MEG8* in cases with upd(14)pat/mat-like phenotypes. Thus, the deletion has caused a relatively mild upd(14)pat phenotype after maternal transmission and upd(14)mat-like phenotype with severe short stature after paternal transmission.

The results are similarly explained by the above notion. In case III-1, loss of the IG-DMR from the maternally derived chromosome would have caused paternalization of the imprinted domain. However, since *DLK1* is deleted from the maternally inherited chromosome, *DLK1* should be present in a single active copy, as

Table 2 (Epi)genotype-phenotype correlations in patients with upd(14)mat-like phenotypes

	Upd(14)mat-like phenotype positive patients				Upd(14)mat patients	Normal subjects
	Deletions			Epimutations		
	Cases 9 and 10 ref. 8	Case 11 ref. 8	Case 12 ref. 27	Cases 13–17 ref. 8, 25, 26	(n = 28) ref. 8	
Phenotype						
Facial features	+	+	-	3/5	68%	-
Low birth weight	+	+	+	5/5	85%	-
Short stature	+	+[a]	+	4/5	85%	-
Early onset of puberty	+	-	+	4/4	85%	-
Obesity	- and +	+	-	3/5	43%	-
Small hands	-	-	+	5/5	89%	-
Hypotonia	-	-	+	5/5	89%	-
Developmental delay	-	-	+	2/5	37%	-
Actual gene dosage						
DLK1	1	1	1	2	2	2
GTL2	1	1	1	2	2	2
RTL1	2	1	1	2	2	2
RTL1as	2	1	1	2	2	2
MEG8	2	1	1	2	2	2
DIO3	2	2	2	2	2	2
Predicted expressed gene dosage[b]						
DLK1	0	0	0	0	0	1
GTL2	1	1	1	2	2	1
RTL1	1	0	0	0	0	1
RTL1as	1	1	1	2	2	1
MEG8	1	1	1	2	2	1
DIO3	1	1	1	0	0	1

[a]Severe short stature. [b]Primarily based on the mouse data of targeted IG-DMR deletion.[6]

in normal individuals. By contrast, while *RTL1* is also present in a single copy, the expression dosage of *RTL1* should be 2.5–3.0 times higher than the normal individuals because of the absence of functional *RTL1as*. Thus, it appears that moderately increased *RTL1* dosage is essential for the development of a relatively mild upd(14) pat phenotype.

In the mother (II-2), there should be no alteration of the imprinting status because of loss of the IG-DMR from the paternally derived chromosome. Thus, the upd(14)mat-like with severe short stature phenotype would simply be ascribed to the loss of *DLK1* and *RTL1* from the paternally derived chromosome.

Deletions affecting the maternally derived 14q32.2 imprinted region. We have also identified two deletions of maternal origin, i.e., a ~475 kb deletion involving the IG-DMR, the *GTL2*-DMR, *GTL2*, *RTL1*, *RTL1as* and *MEG8* and a ~6.5 Mb deletion involving the whole imprinted region in patients with relatively mild upd(14) pat-like phenotype[8] (cases 4 and 5 in Table 1). The phenotype would also be explained by the moderately increased *RTL1* dosage, as in the case III-1 of family B.

Deletions affecting the paternally derived 14q32.2 imprinted region. Buiting et al.[27] have recently identified a ~1 Mb deletion involving *DLK1*, the IG-DMR, the *GTL2*-DMR, *GTL2*, *RTL1*, *RTL1as*, *MEG8* and 14 non-imprinted genes proximal to the imprinted region in a patient with upd(14)mat-like phenotype and severe mental retardation (cases 12 in Table 2). Molecular data in this patient and her mother are consistent with the microdeletion occurring in the paternally derived chromosome, although it remains unknown whether the microdeletion is also present in the father o a de novo abnormality. The upd(14)mat-like phenotype would be consistent with loss of *DLK1* and *RTL1* from the paternally derived chromosome. In addition, severe mental retardation would be due to loss of multiple non-imprinted genes.

Epimutations (hypermethylated DMRs of maternal origin). We have identified three sporadic patients with typical upd(14) pat phenotype and hypermethylated DMRs (epimutations)[8] (cases 6–8 in Table 1). In particular, genotyping analysis for a SNP within the IG-DMR (CG4) confirmed hypermethylation of the usually hypomethylated DMRs of maternal origin. The results are explained by assuming that the hypermethylation of the maternally inherited IG-DMR has caused paternalization of the imprinted region, as in the loss of IG-DMR of maternal origin. In this case, since the expression pattern of the imprinted domain would be comparable to those in upd(14)pat, with 4–5 times of *RTL1* expression dosage, this explains the development of typical upd(14)pat phenotype in these patients.

Epimutations (hypomethylated DMRs of paternal origin). This type of epimutations have been detected in five sporadic patients with upd(14)mat-compatible phenotype[9] (cases 13–17 in Table 2).

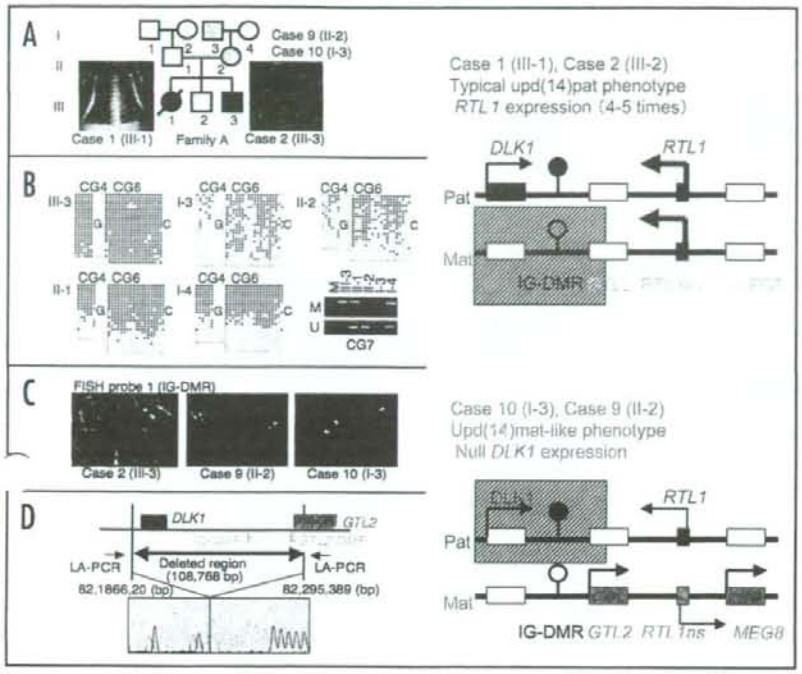

Figure 2. Family A. (A) The pedigree. Cases III-1 (deceased) and III-3 have typical upd(14)pat phenotype, and cases I-3 and II-2 exhibit upd(14)mat-like phenotype. (B) Methylation analysis of the DMRs. The IG-DMR (CG4 and CG6) and the *GTL2*-DMR (CG7) are severely hypermethylated in case III-3 and grossly hypomethylated in cases I-3 and II-2. For the IG-DMR, each lane indicates a single clone, and each circle denotes a CpG island; filled and open circles represent methylated and unmethylated cytosines, respectively. For the *GTL2*-DMR (CG7), methylated allele-specific primers (M) and unmethylated allele-specific primers (U) have been utilized. (C) FISH analysis for the IG-DMR. Heterozygous microdeletion is identified in cases III-3, II-2 and I-3. (D) Direct sequencing for a long and accurate (LA)-PCR product, demonstrating a ~109 kb deletion in cases III-1, II-2 and I-3. The predicted gene dosages are indicated on the right part.

Since clinical features are comparable between epimutation positive patients and upd(14)mat patients, this suggests that the hypomethylation of the paternally inherited IG-DMR has resulted in maternalization of the imprinted region, leading to the development of upd(14)mat-like phenotype.

Placental analysis. Since virtually all the imprinted genes studied to date are expressed in the placenta,[12,15] we examined placental samples obtained from case III-3 in family A with the microdeletion (case 2 in Table 1) and from one case with epimutation (hypermethylation) (case 8 in Table 1), as well as from a upd(14)pat patient and a nearly gestational age-matched control subject.[8] We could also obtain three sets of samples consisting of cDNA and genomic DNA of normal fresh placenta and leukocyte genomic DNA of the mother.

Consequently, we have shown the following: (1) monoallelic paternal *DLK1* expression and maternal *GTL2* expression in the placentas (the genotyping results were not informative for other imprinted genes); (2) paternalization of the maternally inherited imprinted region with markedly elevated *RTL1* expression dosage in case III-3 of family A (case 2) and one case with epimutation (case 8); (3) a parental origin dependent differential methylation pattern of the IG-DMR and grossly hypomethylated *GTL2*-DMR (the results are consistent with the IG-DMR being the germline derived DMR and the *GTL2*-DMR being the secondary DMR, because the germline derived DMRs are delineated as DMRs in the placentas as well as in the embryo, whereas the secondary DMRs, though they behave as DMRs in the embryo, are rather hypomethylated irrespective of the parental origin in the placentas);[6,28-30] and (4) characteristic histological findings such as proliferation of dilated and congested chorionic villi. These findings imply that the phenotypic development is closely associated with altered expression dosage of the imprinted genes in both the embryo and the placenta, and that epigenetic control is different between the embryo and the placentas in the human as well as in the mouse, and between the human and the mouse placentas with maternally derived deletion of the IG-DMR.

Unresolved Matters

Despite the above progress, many matters remain to be clarified. First, the precise mechanisms involved in the imprinting regulation are largely unknown, although several possibilities have been put forward recently.[31] Thus, it remains to be determined why *PEGs* are expressed when the DMRs are methylated and *MEGs* are expressed when the DMRs are unmethylated, and how the methylation pattern of the IG-DMR and the *GTL2*-DMR controls all the imprinted genes in this domain. Recent work indicates that the methylated IG-DMR influences chromatin topology at the locus which may facilitate *PEG* activity on the paternally derived chromosome.[32] Evidence suggests that, on the maternal chromosome, the noncoding *MEGs* can be splice variants of a single giant gene regulated by the methylation status of the *GTL2*-DMR.[33,34] A causal role for maternally expressed *Gtl2* associated ncRNA transcription in the cis-acting repression of the protein coding genes is one possible regulatory scenario. Furthermore, the effects of the *GTL2*-DMR deletion alone on expression and clinical consequences remain unknown. Targeted deletion of the *Gtl2*-DMR has not been reported to date. Furthermore, the function of *RTL1as* in repressing *RTL1* expression remains to be confirmed in the human. Indeed, if the repressor function is stronger in the human than in the mouse, this would lead to even more pronounced effects on *RTL1* transcript levels in the human patients with upd(14)pat, microdeletions and epimutations. This may underlie the phenotypic difference between the human and the mouse paternal disomy. Finally, several issues such as the biological functions of most *MEGs/Megs*, the function of the multiple microRNAs in the human imprinted region, the imprinting status of human *DIO3*, the mechanisms leading to epimutations, and the mechanisms involved in the placental imprinting regulation also remain to be elucidated. These matters await further investigations.

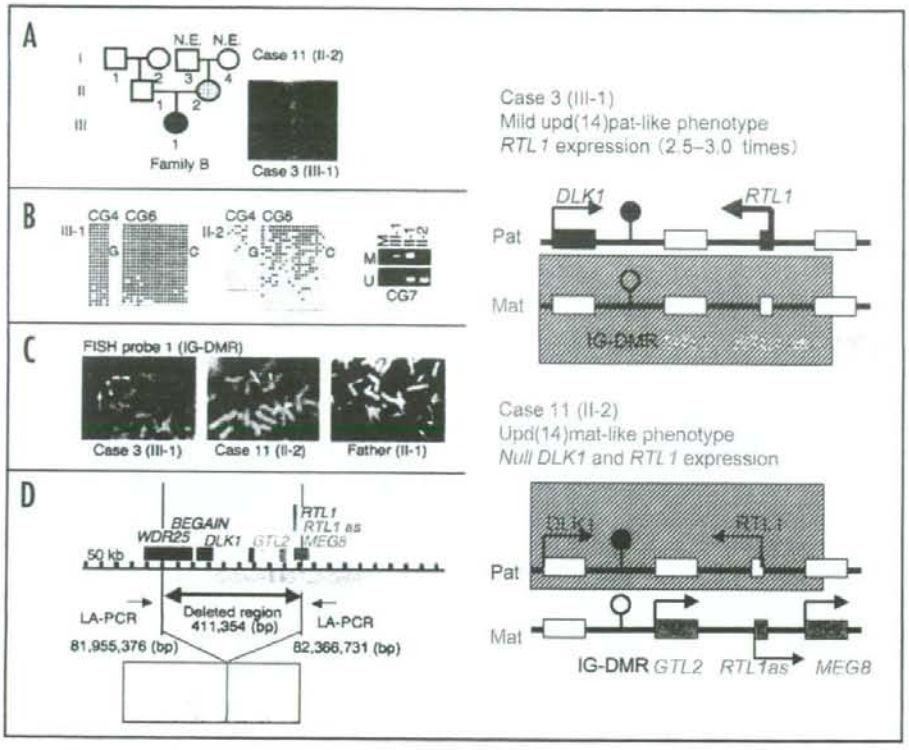

Figure 3. Family B. (A) The pedigree. Cases III-1 show upd(14)pat-like phenotype, and cases I-3 and II-2 exhibit upd(14)mat-like phenotype. (B) Methylation analysis of the DMRs. The IG-DMR (CG4 and CG6) and the *GTL2*-DMR (CG7) are severely hypermethylated in case III-3 and grossly hypomethylated in case II-2. (C) FISH analysis for the IG-DMR. Heterozygous microdeletion is identified in cases III-1 and II-2. (D) Direct sequencing for an LA-PCR product, demonstrating a ~109 kb deletion in cases III-1 and II-2. The predicted gene dosages are indicated on the right part.

References

1. Cavaille J, Seitz H, Paulsen M, Ferguson-Smith AC, Bachellerie JP. Identification of tandemly-repeated C/D snoRNA genes at the imprinted human 14q32 domain reminiscent of those at the Prader-Willi/Angelman syndrome region. Hum Mol Genet 2002; 11:1527-38.
2. Charlier C, Segers K, Wagenaar D, Karim L, Berghmans S, Jaillon O, Shay T, Weissenbach J, Cockett N, Gyapay G, Georges M. Human-ovine comparative sequencing of a 250-kb imprinted domain encompassing the callipyge (*clpg*) locus and identification of six imprinted transcripts: *DLK1, DAT, GTL2, PEG11, antiPEG11* and *MEG8*. Genome Res 2001; 11:850-62.
3. Tsai CE, Lin SP, Ito M, Takagi N, Takada S, Ferguson-Smith AC. Genomic imprinting contributes to thyroid hormone metabolism in the mouse embryo. Curr Biol 2002; 12:1221-26.
4. Li E, Beard C, Jaenisch R. Role for DNA methylation in genomic imprinting. Nature 1993; 366:362-5.
5. Paulsen M, Takada S, Youngson NA, Benchaib M, Charlier C, Segers K, Georges M, Ferguson-Smith AC. Comparative sequence analysis of the imprinted *Dlk1-Gtl2* locus in three mammalian species reveals highly conserved genomic elements and refines comparison with the *Igf2-H19* region. Genome Res 2001; 11:2085-94.
6. Lin SP, Youngson N, Takada S, Seitz H, Reik W, Paulsen M, Cavaille J, Ferguson-Smith AC. Asymmetric regulation of imprinting on the maternal and paternal chromosomes at the *Dlk1-Gtl2* imprinted cluster on mouse chromosome 12. Nat Genet 2003; 35:97-102.
7. Murphy SK, Wylie AA, Coveler KJ, Cotter PD, Papenhausen PR, Sutton VR, Shaffer LG, Jirtle RL. Epigenetic detection of human chromosome 14 uniparental disomy. Hum Mutat 2003; 22:92-7.
8. Kagami M, Sekita Y, Nishimura G, Irie M, Kato F, Okada M, Yamamori S, Kishimoto H, Nakayama M, Tanaka Y, Matsuoka K, Takahashi T, Noguchi M, Tanaka Y, Masumoto K, Utsunomiya T, Kouzan H, Komatsu Y, Ohashi H, Kurosawa K, Kosaki K, Ferguson-Smith AC, Ishino F, Ogata T. Deletions and epimutations affecting the human 14q32.2 imprinted region in individuals with paternal and maternal upd(14)-like phenotypes. Nat Genet 2008; 40:237-42.
9. Kotzot D. Maternal uniparental disomy 14 dissection of the phenotype with respect to rare autosomal recessively inherited traits, trisomy mosaicism, and genomic imprinting. Ann Genet 2004; 47:251-60.
10. Gunay-Aygun M, Schwartz S, Heeger S, O'Riordan MA, Cassidy SB. The changing purpose of Prader-Willi syndrome clinical diagnostic criteria and proposed revised criteria. Pediatrics 2001; 108:92.
11. Bittel DC, Butler MG. Prader-Willi syndrome: clinical genetics, cytogenetics and molecu' biology. Expert Rev Mol Med 2005; 7:1-20.
12. Coan PM, Burton GJ, Ferguson-Smith AC. Imprinted genes in the placenta. Placenta 2005; 26:10-20.
13. Fowden AL, Sibley C, Reik W, Constancia M. Imprinted genes, placental development and fetal growth. Horm Res 2006; 65:50-8.
14. Kagami M, Yamazawa K, Matsubara K, Mitsuo N, Ogata T. Placentomegaly in paternal uniparental disomy for human chromosome 14. Placenta 2008.
15. Kaneko-Ishino T, Kohda T, Ishino F. The regulation and biological significance of genomic imprinting in mammals. J Biochem 2003; 133:699-711.
16. Lin SP, Coan P, da Rocha ST, Seitz H, Cavaille J, Teng PW, Takada S, Ferguson-Smith AC. Differential regulation of imprinting in the murine embryo and placenta by the Dlk1-Dio3 imprinting control region. Development 2007; 134:417-26.
17. Georgiades P, Watkins M, Surani MA, Ferguson-Smith AC. Parental origin-specific developmental defects in mice with uniparental disomy for chromosome 12. Development 2000; 127:4719-28.
18. Takada S, Paulsen M, Tevendale M, Tsai CE, Kelsey G, Cattanach BM, Ferguson-Smith AC. Epigenetic analysis of the Dlk1-Gtl2 imprinted domain on mouse chromosome 12: implications for imprinting control from comparison with Igf2-H19. Hum Mol Genet 2002; 11:77-86.
19. Seitz H, Youngson N, Lin SP, Dalbert S, Paulsen M, Bachellerie JP, Ferguson-Smith AC, Cavaillé J. Imprinted microRNA genes transcribed antisense to a reciprocally imprinted retrotransposon-like gene. Nat Genet 2003; 34:261-2.
20. Davis E, Caiment F, Tordoir X, Cavaillé J, Ferguson-Smith A, Cockett N, Georges M, Charlier C. RNAi-mediated allelic trans-interaction at the imprinted Rtl1/Peg11 locus. Curr Biol 2005; 15:743-9.
21. Moon YS, Smas CM, Lee K, Villena JA, Kim KH, Yun EJ, Sul HS. Mice lacking paternally expressed Pref-1/Dlk1 display growth retardation and accelerated adiposity. Mol Cell Biol 2002; 22:5585-92.

22. Sekita Y, Wagatsuma H, Nakamura K, Ono R, Kagami M, Wakisaka N, Hino T, Suzuki-Migishima R, Kohda T, Ogura A, Ogata T, Yokoyama M, Kaneko-Ishino T, Ishino F. Role of retrotransposon-derived imprinted gene, Rtl1, in the feto-maternal interface of mouse placenta. Nat Genet 2008; 40:243-8.
23. Hernandez A, Martinez ME, Fiering S, Galton VA, St Germain D. Type 3 deiodinase is critical for the maturation and function of the thyroid axis. J Clin Invest 2006; 116:476-84.
24. Sekita Y, Wagatsuma H, Irie M, Kobayashi S, Kohda T, Matsuda J, Yokoyama M, Ogura A, Schuster-Gossler K, Gossler A, Ishino F, Kaneko-Ishino T. Aberrant regulation of imprinted gene expression in Gtl2lacZ mice. Cytogenet Genome Res 2006; 113:223-9.
25. Temple IK, Shrubb V, Lever M, Bullman H, Mackay DJ. Isolated imprinting mutation of the DLK1/GTL2 locus associated with a clinical presentation of maternal uniparental disomy of chromosome 14. J Med Genet 2007; 44:637-40.
26. Hosoki K, Ogata T, Kagami M, Tanaka T, Saitoh S. Epimutation (hypomethylation) affecting the chromosome 14q32.2 imprinted region in a girl with upd(14)mat-like phenotype. Eur J Hum Genet 2008; 16:1019-23.
27. Buiting K, Kanber D, Martin-Subero JI, Lieb W, Terhal P, Albrecht B, Purmann S, Gross S, Lich C, Siebert R, Horsthemke B, Gillessen-Kaesbach G. Clinical features of maternal uniparental disomy 14 in patients with an epimutation and a deletion of the imprinted DLK1/GTL2 gene cluster. Hum Mutat 2008.
28. Monk D, Arnaud P, Apostolidou S, Hills FA, Kelsey G, Stanier P, Feil R, Moore GE. Limited evolutionary conservation of imprinting in the human placenta. Proc Natl Acad Sci USA 2006; 103:6623-8.
29. Lewis A, Mitsuya K, Umlauf D, Smith P, Dean W, Walter J, Higgins M, Feil R, Reik W. Imprinting on distal chromosome 7 in the placenta involves repressive histone methylation independent of DNA methylation. Nat Genet 2004; 36:1291-5.
30. Umlauf D, Goto Y, Cao R, Cerqueira F, Wagschal A, Zhang Y, Feil R. Imprinting along the Kcnq1 domain on mouse chromosome 7 involves repressive histone methylation and recruitment of Polycomb group complexes. Nat Genet 2004; 36:1296-300.
31. da Rocha ST, Edwards CA, Ito M, Ogata T, Ferguson-Smith AC. Genomic imprinting at the mammalian Dlk1-Dio3 domain. Trends Genet 2008; 24:306-16.
32. Braem C, Recolin B, Rancourt RC, Angiolini C, Barthès P, Branchu P, Court F, Cathala G, Ferguson-Smith AC, Forné T. Genomic MAR and 3C-qPCR assays identify novel putative regulatory elements at the imprinted Dlk1/Gtl2 locus. J Biol Chem 2008.
33. Tierling S, Dalbert S, Schoppenhorst S, Tsai CE, Oliger S, Ferguson-Smith AC, Paulsen M, Walter J. High-resolution map and imprinting analysis of the Gtl2-Dnchc1 domain on mouse chromosome 12. Genomics 2006; 87:225-35.
34. Mikkelsen TS, Ku M, Jaffe DB, Issac B, Lieberman E, Giannoukos G, Alvarez P, Brockman W, Kim TK, Koche RP, Lee W, Mendenhall E, O'Donovan A, Presser A, Russ C, Xie X, Meissner A, Wernig M, Jaenisch R, Nusbaum C, Lander ES, Bernstein BE. Genome-wide maps of chromatin state in pluripotent and lineage-committed cells. Nature 2007; 448:553-60.

American Journal of Medical Genetics Part A 146A:2162–2163 (2008)

Research Letter

SOX10 Mutation in Waardenburg Syndrome Type II

Manami Iso,[1] Maki Fukami,[1] Reiko Horikawa,[2] Noriyuki Azuma,[3] Nobuko Kawashiro,[4] and Tsutomu Ogata[1]*

[1]Department of Endocrinology and Metabolism, National Research Institute for Child Health and Development, Tokyo, Japan
[2]Division of Endocrinology and Metabolism, National Center for Child Health and Development, Tokyo, Japan
[3]Division of Ophthalmology, National Center for Child Health and Development, Tokyo, Japan
[4]Division of Otorhinolaryngology, National Center for Child Health and Development, Tokyo, Japan

Received 20 February 2008; Accepted 3 May 2008

How to cite this article: Iso M, Fukami M, Horikawa R, Azuma N, Kawashiro N, Ogata T. 2008. *SOX10* mutation in Waardenburg syndrome type II. Am J Med Genet Part A 146A:2162–2163.

To the Editor:

Waardenburg syndrome (WS) is a congenital developmental disorder characterized by sensorineural hearing loss and abnormal pigmentation of the eye, hair, and skin [Jones, 2006]. This condition is divided into four types [reviewed in Jones, 2006; Bondurand et al., 2007]. Type I WS (WS1) consists of dystopia canthorum and broad nasal root, and is almost exclusively caused by heterozygous mutations of *PAX3*. Type II WS (WS2) lacks the dystopia canthorum and results from heterozygous mutations of *MITF* (WS2A) in ~15% of patients and homozygous deletions of *SNAI2* (WS2D) in two patients. Type III WS (WS3) (Klein–Waardenburg syndrome), a severe form of WS1, is associated with upper limb defects, and is ascribed to heterozygous or homozygous mutations of *PAX3*. Type IV WS (WS4) (Shah–Waardenburg syndrome) is characterized by Hirschsprung disease, and is caused by heterozygous or homozygous mutations of *EDNRB* or its ligand *EDN3*, or by heterozygous mutations of *SOX10*.

Thus, the underlying causes remain to be clarified in most of the WS2 patients. While a WS2 locus is mapped to chromosome 1p (WS2B) [Lalwani et al., 1994] and chromosome 8q23 (WS2C) [Selicorni et al., 2002], a causative gene(s) has not been identified from these regions. In this regard, Bondurand et al. [2007] have recently identified *SOX10* deletions in patients with WS2, implying that *SOX10* abnormalities can cause WS2 (WS2E) as well as WS4. Here, we describe another case of WS2E caused by heterozygous *SOX10* mutation.

This Japanese girl was born to nonconsanguineous healthy parents at 41 weeks of gestation after an uncomplicated pregnancy and delivery. At birth, her length was 49.6 cm (+0.6 SD), and her weight 3.4 kg (+0.1 SD). She was found to have light blue eyes, and referred to us at 12 days of age. She manifested hypopigmented irides and a piece of white forelock, but lacked dystopia canthorum, broad nasal root, and Hirschsprung disease. Ophthalmologic examinations revealed bilateral ocular albinism with hypopigmented fundus and hypochromic iris. At 3.5 months of age, auditory brainstem response was performed because of poor responses to sounds, showing bilateral severe sensorineural deafness (hearing level, 90 dB bilaterally). Brain computed tomography showed no abnormal finding. On the basis of the above findings, she was diagnosed as having WS2.

After obtaining written informed consent, direct sequencing was performed for leukocyte genomic DNA of this patient, detecting no abnormality in the coding sequences of *PAX3*, *MITF*, and *SNAI2*. However, we identified a heterozygous *SOX10* frameshift mutation (c.506delC) on exon 4 that is predicted to result in a premature termination at the 284th amino acid (p.Pro169fsX284) (Fig. 1A). The primer sequences and the annealing temperature used were: exon 3, GTTGGACTCTTTGCGAGGAC and ATCCACCCGAAGCTAGAGG (58°C); exon 4, AGCCCCTCTGCTGTCCTCT and CACCCTCAGCTCTGTCATCA (60°C); and exon 5, CTAACCTGCTTCCCCCTTG and CAAGGAACAGGGCACACAG (58°C). This frameshift mutation located within the high mobility group (HMG) DNA-binding domain, and removed the C-terminal part of the HMG domain and the whole transactivation domain. This mutation is predicted to destroy an *Nci*I restriction site, and

*Correspondence to: Tsutomu Ogata, M.D., Department of Endocrinology and Metabolism, National Research Institute for Child Health and Development, Tokyo 157-8535, Japan. E-mail: tomogata@nch.go.jp

Published online 14 July 2008 in Wiley InterScience (www.interscience.wiley.com)
DOI 10.1002/ajmg.a.32403

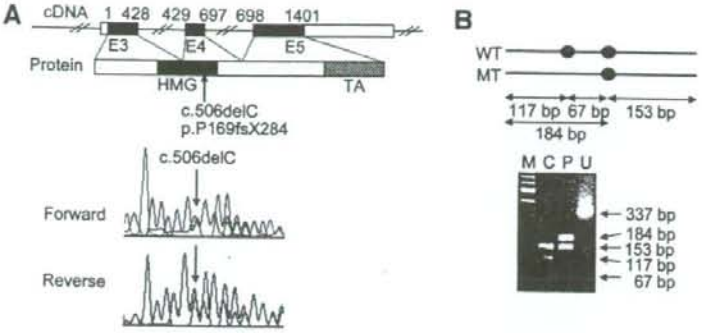

FIG. 1. Mutational analysis of *SOX10*. **A**: Direct sequencing of exon 4. Shown on the upper part is a schematic representation indicating the coding exons 3–5 (E3–E5) and the functional domains. For the *SOX10* cDNA, the black and white areas denote the coding regions and the untranslated regions, respectively, and the Arabic numbers indicate the cDNA sequence encoded by each exon. For the SOX10 protein, the gray and striped squares represent the high mobility group (HMG) DNA-binding domain and the transactivating (TA) domain. Electrochromatograms (forward and reverse) indicate a heterozygous c.506delC mutation on exon 4. **B**: Restriction enzyme analysis. The black circles represent *Nci*I restriction sites. PCR products contain naturally occurring two *Nci*I sites on the wild-type (WT) exon 4, and one of the two *Nci*I sites is predicted to be destroyed on the mutant (MT) exon 4. After *Nci*I digestion, WT sequence specific 117 and 67 bp bands only are found for a control subject (C), whereas WT specific 117 bp and 67 bp bands and a MT specific 184 bp band are shown for the patient (P). M: size marker; and U: undigested PCR product (337 bp).

this was confirmed by the *Nci*I digestion of the corresponding PCR products (Fig. 1B). While the parents postponed the decision to have the genetic testing, this mutation was absent in 100 control subjects.

The results provide further support for the notion that WS2 can be caused by heterozygous abnormalities of *SOX10* (WS2E). In this regard, a *SOX10* frameshift mutation (c.1076–1077delGA, p.Thr360fsX399) has been identified not only in a patient with a typical WS4 but also in the mother with an apparently WS2-compatible deafness and white forelock only phenotype [Pingault et al., 1998]. In addition, another *SOX10* missense mutation (p.Ser135Thr) has also been detected in a patient with "Yemenite deaf-blind hypopigmentation syndrome" mimicking WS2 [Bondurand et al., 1999]. These findings, together with *SOX10* deletions in patients with WS2 [Bondurand et al., 2007], imply that heterozygous *SOX10* abnormalities lead to not only WS4 but also to the WS2 phenotype. Such phenotypic variability would not be unexpected, because it is known that heterozygous mutations of developmental genes are usually associated with wide range of expressivity and penetrance [Fisher and Scambler, 1994]. In addition, the position of the frameshift mutation on exon 4 may also be relevant to the lack of associated features, because *SOX10* mutations residing on the last exon frequently lead to more severe phenotypes such as chronic intestinal pseudo-obstruction and/or neurological features, probably due to escape from the nonsense mediated mRNA decay [Pingault et al., 2000, 2002; Inoue et al., 2004].

REFERENCES

Bondurand N, Kuhlbrodt K, Pingault V, Enderich J, Sajus M, Tommerup N, Warburg M, Hennekam RC, Read AP, Wegner M, Goossens M. 1999. A molecular analysis of the yemenite deaf-blind hypopigmentation syndrome: SOX10 dysfunction causes different neurocristopathies. Hum Mol Genet 8:1785–1789.

Bondurand N, Dastot-Le Moal F, Stanchina L, Collot N, Baral V, Marlin S, Attie-Bitach T, Giurgea I, Skopinski L, Reardon W, Toutain A, Sarda P, Echaieb A, Lackmy-Port-Lis M, Touraine R, Amiel J, Goossens M, Pingault V. 2007. Deletions at the SOX10 gene locus cause Waardenburg syndrome types 2 and 4. Am J Hum Genet 8:1169–1185.

Fisher E, Scambler P. 1994. Human haploinsufficiency—One for sorrow, two for joy. Nat Genet 7:5–7.

Inoue K, Khajavi M, Ohyama T, Hirabayashi S, Wilson J, Reggin JD, Mancias P, Butler IJ, Wilkinson MF, Wegner M, Lupski JR. 2004. Molecular mechanism for distinct neurological phenotypes conveyed by allelic truncating mutations. Nat Genet 36:361–369.

Jones KL. 2006. Waardenburg syndrome, types I and II. In: Jones KL, editor. Smith's recognizable patterns of human malformation. Philadelphia: Elseview Saunders. p 278–279.

Lalwani AK, Baldwin CT, Morell R, Friedman TB, San Agustin TB, Milunsky A, Adair R, Asher JH, Wilcox ER, Farrer LA. 1994. A locus for Waardenburg syndrome type II maps to chromosome 1p13.3–2.1. Am J Hum Genet 55:A14.

Pingault V, Bondurand N, Kuhlbrodt K, Goerich DE, Préhu MO, Puliti A, Herbarth B, Hermans-Borgmeyer I, Legius E, Matthijs G, Amiel J, Lyonnet S, Ceccherini I, Romeo G, Smith JC, Read AP, Wegner M, Goossens M. 1998. SOX10 mutations in patients with Waardenburg-Hirschsprung disease. Nat Genet 18:171–173.

Pingault V, Guiochon-Mantel A, Bondurand N, Faure C, Lacroix C, Lyonnet S, Goossens M, Landrieu P. 2000. Peripheral neuropathy with hypomyelination, chronic intestinal pseudo-obstruction and deafness: A developmental "neural crest syndrome" related to a SOX10 mutation. Ann Neurol 48:671–676.

Pingault V, Girard M, Bondurand N, Dorkins H, Van Maldergem L, Mowat D, Shimotake T, Verma I, Baumann C, Goossens M. 2002. SOX10 mutations in chronic intestinal pseudo-obstruction suggest a complex physiopathological mechanism. Hum Genet 111:198–206.

Selicorni A, Guerneri S, Ratti A, Pizzuti A. 2002. Cytogenetic mapping of a novel locus for type II Waardenburg syndrome. Hum Genet 110:64–67.

Available online at www.sciencedirect.com
ScienceDirect
PLACENTA
Placenta 29 (2008) 760–761

Letter to the Editor

Placentomegaly in Paternal Uniparental Disomy for Human Chromosome 14

Sir,

Paternal uniparental disomy for chromosome 14 (upd (14)pat) causes a unique phenotype characterized by polyhydramnios, dysmorphic features, small bell-shaped thorax, and abdominal wall defect [1]. Since chromosome 14q32.2 region harbors several paternally expressed genes (*PEGs*) such as *DLK1* and *RTL1* and maternally expressed genes (*MEGs*) such as *GTL2* (alias, *MEG3*), *RTL1as* (*RTL1 antisense*), and *MEG8*, upd(14)pat phenotype is ascribed to the increased dosage of active *PEGs* and the absence of functional *MEGs* [2]. In this regard, we have suggested that increased *RTL1* dosage plays a major role in the development of upd(14)pat phenotype, on the basis of epigenotype–phenotype correlations in eight patients with upd(14)pat-like phenotypes with various microdeletions or epimutations affecting the imprinted region [2].

Virtually, all the imprinted genes studied to date are expressed in the placenta [3]. This is consistent with the notion that imprinted genes are identified from placental mammals and play a pivotal role in placental growth and development. Indeed, placental hypoplasia has been identified in SRS patients with upd(7)mat [4] or epimutations of the *H19*-differentially methylated region (DMR) [5], and placentomegaly has been described in Beckwith–Wiedemann syndrome (BWS) patients with upd(11p15.5)pat [6]. These findings, together with the results of knockout mouse experiments for imprinted genes [3], imply that placental growth is promoted by *PEGs* and suppressed by *MEGs*. However, the placental weight data remain poor in upd(14)pat, although the presence of placentomegaly has been mentioned briefly [2].

Thus, we examined placental weights in 10 patients with upd (14)pat (Table 1). This study was approved by the Institutional Review Board Committee at National Center for Child Health and Development, and performed after obtaining written informed consent. Cases 1–3 have previously been reported with no description on the placental weights [1], and cases 4–10 are hitherto unreported patients. Cases 1–10 were ascertained because of the pathognomonic bell-shaped thorax, and were found to have typical upd(14)pat phenotypes; although polyhydramnios was apparently absent in case 5, this would be due to very premature (24 weeks of gestation) delivery by an emergent Caesarean section for severe fetal distress (detailed clinical features of each case are available on request). Karyotype was normal in the nine cases examined. Microsatellite analysis was performed for 14 loci dispersed on chromosome 14 using leukocyte genomic DNA samples obtained from cases 1–10 and all of the parents, indicating segmental paternal isodisomy in case 1, full paternal isodisomy in cases 2–8, mixture of paternal heterodisomy for the proximal to middle part of 14q and isodisomy for the distal part of 14q in case 9, and full paternal heterodisomy in case 10 (the genotyping data are available on request). Thus, the 14q32.2 imprinted region was present in an isodisomic status in cases 1–9 and in a heterodisomic status in case 10. Furthermore, methylation analyses for the IG-DMR and *GTL2*-DMR [2] confirmed upd(14)pat in cases 1–10.

The placental weights in cases 1–10 are shown in Table 1. They were obtained from the hospital records, and were assessed by the Japanese placental weight data collected during the years 1981–1984 [7] and by those collected from January 2006 to April 2008 (our unpublished observation). The placental weights were above the mean in all cases and above the +2 SD of the mean in most cases, while there was a considerable degree of variation. In particular, they were ~2 times increased in cases 1, 4, and 8 with paternal isodisomy and in case 10 with paternal heterodisomy. Unfortunately, since placental tissues were not preserved, histological examination could not be performed, except for the placenta of case 3 which was characterized by proliferation of dilated and congested chorionic villi [the histological findings have been reported in Ref. [2]].

The present study showed the presence of placentomegaly in upd(14)pat. In this context, the human 14q32.2 imprinted region is highly conserved on the distal part of the mouse chromosome 12, and paternal uniparental disomy for chromosome 12 (PatDi(12)) results in placentomegaly, whereas MatDi(12) leads to placental hypoplasia [8]. In addition, mice with 2.5–3.0 times of *Rtl1* expression caused by maternally derived *Rtl1as* deletion have placentomegaly, whereas mice with null *Rtl1* expression caused by paternally derived *Rtl1* deletion have placental hypoplasia [9]. Collectively, these findings suggest that *RTL1/Rtl1* expression dosage plays a critical role in the placental growth. Consistent with this, mouse Rtl1 protein is identified exclusively in the labyrinth zone of the placenta [9].

Several points should be made in reference to the placentomegaly in upd(14)pat. First, the degree of placentomegaly was considerably variable in cases 1–10. This may imply

0143-4004/$ - see front matter
doi:10.1016/j.placenta.2008.06.001

Table 1
Summary of patients with paternal uniparental disomy for chromosome 14

	Case 1	Case 2	Case 3	Case 4	Case 5	Case 6	Case 7	Case 8	Case 9	Case 10
Sex	Female	Male	Female	Female	Male	Male	Female	Female	Male	Male
Polyhydramnios	+	+	+	+	−	+	+	+	+	+
Dysmorphic features	+	+	+	+	+	+	+	+	+	+
Bell-shaped thorax	+	+	+	+	+	+	+	+	+	+
Abdominal wall defects	+	+	+	+	+	+	+	+	+	+
Karyotype	46,XX	N.E.	46,XX	46,XX	46,XY	46,XY	46,XX	46,XX	46,XY	46,XY
Pathogenesis	Seg-iso	Full-iso	Full-iso	Full-iso	Full-iso	Full-iso	Full-iso	Full-iso	Hetero/Iso	Full-hetro
Imprinted region	Isodisomy	Isodisomy	Isodisomy	Isodisomy	Isodisomy	Isodisomy	Isodisomy	Isodisomy	Isodisomy	Heterodisomy
Gestational age (wks)	36	34	32	34	24	36	37	36	34	37
Placental weight (g)	1108	556	635	1108	278	570	750	970	640	1030
Placental weight (%)[a]	227	114	161	227	114	117	142	198	131	195
Placental weight (SDS)[b]	+6.1	+1.6	+3.4	+8.0	N.A.	+0.9	+2.4	+4.9	+2.6	+5.3

N.E.: not examined; SDS: standard deviation score; and N.A.: not available.

[a] Evaluated by the Japanese placental weight data obtained between the years 1981–1984 [7]; the mean placental weight is 244 g for 21–24 weeks of gestation ($n = 40$), 300 g for 25–28 weeks ($n = 181$), 394 g for 29–32 weeks ($n = 333$), 489 g for 33–36 weeks ($n = 483$), and 527 g for 37–40 weeks ($n = 2282$).

[b] Assessed by the Japanese placental weight data collected between January 2006 and April 2008; the placental weight (mean ± SD) is not available for 24 we of gestation, 375 ± 75 g for 32 weeks ($n = 7$), 423 ± 85 g for 34 weeks ($n = 15$), 478 ± 101 g for 36 weeks ($n = 28$), and 510 ± 98 g for 37 weeks ($n = 36$).

a relatively weak placental growth regulation in imprinting disorders, which could be related to the differential imprinting regulation between bodies and placentas [10]. Second, placentomegaly may exaggerate the amniotic fluid production, leading to the development of polyhydramnios. In support of this, the association of placentomegaly with polyhydramnios has also been reported in BWS [11]. Third, although the degree of placentomegaly was apparently irrelevant to the type of disomy, it remains to be clarified whether placental phenotype is somewhat different between patients with isodisomy and those with heterodisomy. Indeed, since heterodisomy is usually caused by trisomy rescue [12], there may be placental confined trisomy that may influence the placental growth and development [12]. In addition, since unmasking of recessive mutations is possible in isodisomy [12], this may lead to a specific phenotype in both the body and the placenta in exceptional patients with paternally derived recessive mutations. Lastly, while placentomegaly appears to be associated with characteristic histological findings [2], further studies are required to define the histological characters in upd(14)pat.

References

[1] Kagami M, Nishimura G, Okuyama T, Hayashidani M, Takeuchi T, Tanaka S, et al. Segmental and full paternal isodisomy for chromosome 14 in three patients: narrowing the critical region and implication for the clinical features. Am J Med Genet A 2005;138:127–32.

[2] Kagami M, Sekita Y, Nishimura G, Irie M, Kato F, Okada M, et al. Deletions and epimutations affecting the human 14q32.2 imprinted region in individuals with paternal and maternal upd(14)-like phenotypes. Nat Genet 2008;40:237–42.

[3] Fowden AL, Sibley C, Reik W, Constancia M. Imprinted genes, placental development and fetal growth. Horm Res 2006;65(Suppl 3):50–8.

[4] Yamazawa K, Kagami M, Ogawa M, Horikawa R, Ogata T. Placental hypoplasia in maternal uniparental disomy for chromosome 7. Am J Med Genet A 2008;146:514–6.

[5] Yamazawa K, Kagami M, Nagai T, Kondoh T, Onigata K, Maeyama K, et al. Molecular and clinical findings and their correlations in Silver–Russell syndrome: implications for a positive role of IGF2 in growth determination and differential imprinting regulation of the IGF2–H19 domain in bodies and placentas. J Mol Med, in press.

[6] Robinson WP, Slee J, Smith N, Murch A, Watson SK, Lam WL, et al. Placental mesenchymal dysplasia associated with fetal overgrowth and mosaic deletion of the maternal copy of 11p15.5. Am J Med Genet A 2007;143:1752–9.

[7] Nakayama M. Reference values of placentas and umbilical cords. In: Nakayama M, editor. Placental pathology. Tokyo: Igaku Shoin; 2001. p. 103–7 [in Japanese].

[8] Georgiades P, Watkins M, Surani MA, Ferguson-Smith AC. Parental origin-specific developmental defects in mice with uniparental disomy for chromosome 12. Development 2000;127:4719–28.

[9] Sekita Y, Wagatsuma H, Nakamura K, Ono R, Kagami M, Wakisaka N, et al. Role of retrotransposon-derived imprinted gene, Rtl1, in the feto-maternal interface of mouse placenta. Nat Genet 2008;40:243–8.

[10] Monk D, Arnaud P, Apostolidou S, Hills FA, Kelsey G, Stanier P, et al. Limited evolutionary conservation of imprinting in the human placenta. Proc Natl Acad Sci U S A 2006;103:6623–8.

[11] Weng EY, Moeschler JB, Graham Jr JM. Longitudinal observations on 15 children with Wiedemann–Beckwith syndrome. Am J Med Genet 1995;56:366–73.

[12] Robinson WP. Mechanisms leading to uniparental disomy and their c. ical consequences. Bioessays 2000;22:452–9.

M. Kagami
K. Yamazawa
K. Matsubara
Department of Endocrinology and Metabolism, National Research Institute for Child Health and Development, Tokyo 157-8535, Japan

N. Matsuo
Department of Pediatrics, Nerima General Hospital, Tokyo, Japan

T. Ogata*
Department of Endocrinology and Metabolism, National Research Institute for Child Health and Development, Tokyo 157-8535, Japan
*Corresponding author. Tel.: +81 3 5494 7025; fax: +81 3 5494 7026.
E-mail address: tomogata@nch.go.jp (T. Ogata)

Accepted 4 June 2008